1305
8042

TECH LIBRARY KAFB, NM
0144610

NATIONAL ADVISORY COMMITTEE FOR AERONAUTICS

TECHNICAL NOTE

No. 1305

EFFECT OF LENGTH-BEAM RATIO ON THE AERODYNAMIC CHARACTERISTICS OF FLYING-BOAT HULLS

By Campbell C. Yates and John M. Riebe

Langley Memorial Aeronautical Laboratory
Langley Field, Va.

Washington
June 1947

AFMDC
TECHNICAL LIBRARY
AFL 2811

TECH LIBRARY KAFB, NM
0144610

NATIONAL ADVISORY COMMITTEE FOR AERONAUTICS

TECHNICAL NOTE NO. 1305

EFFECT OF LENGTH-BEAM RATIO ON THE AERODYNAMIC CHARACTERISTICS OF FLYING-BOAT HULLS

By Campbell C. Yates and John M. Riebe

SUMMARY

A wind-tunnel investigation was made to determine the effect of length-beam ratio on the aerodynamic characteristics of a family of flying-boat hulls in the presence of a wing. The hulls were designed to have approximately the same hydrodynamic performance with respect to spray and resistance characteristics regardless of length-beam ratio.

The investigation indicated a reduction in minimum drag coefficient of 0.0022 (29 percent) with fixed transition when length-beam ratio was extended from 6 to 15. Minimum drag generally occurred in the angle-of-attack range from 2° to 3° for all length-beam ratios. Increasing length-beam ratio from 6 to 15 increased the hull longitudinal stability by an amount corresponding to a rearward aerodynamic-center shift of about $2\frac{1}{2}$ percent mean aerodynamic chord on a flying boat; at an angle of attack of 2° the same change in length-beam ratio increased the hull directional instability by increasing the variation of yawing-moment coefficient with angle of yaw from a value of 0.0009 to a value of 0.0014.

Incorporating a hull step fairing, which extended longitudinally about 9 times the depth of the step at the keel, resulted in a reduction up to 16 percent in minimum drag coefficient.

INTRODUCTION

In view of the requirements for increased range and increased speed in future flying-boat designs, the Langley Laboratory of the NACA is making an investigation of the aerodynamic characteristics of flying-boat hulls as affected by hull dimensions and hull shape.

Hydrodynamic tests have shown that at the same gross load the length-beam ratio may be varied without appreciably altering the hydrodynamic performance with respect to resistance and spray characteristics provided that the product of the beam and the square of the length is held constant. This criterion was used in designing a family of hulls with length-beam ratios of 6, 9, 12, and 15 which are applicable to a flying boat for which gross weight, power, center of gravity, tail length, and all geometries except the hull itself are held constant. The hydrodynamic performance with respect to spray and resistance characteristics would therefore be similar regardless of length-beam ratio in the aforementioned range; thus, the relative aerodynamic performance of the hulls would be an important factor in determining the length-beam ratio used in the flying-boat design.

The present investigation was made in the Langley 300 MPH 7- by 10-foot tunnel to determine the effect of length-beam ratio on the aerodynamic characteristics of the family of hulls previously described. The effect of wing interference is included in these characteristics.

COEFFICIENTS AND SYMBOLS

The results of the tests are presented as standard NACA coefficients of forces and moments. Rolling-moment, yawing-moment, and pitching-moment coefficients are given about the location (30-percent-chord point of wing) shown in figure 1. Except where noted, the wing area, mean aerodynamic chord, and span of a hypothetical flying boat derived from the XPBB-1 flying boat (fig. 2) are used in determining the coefficients and Reynolds number. The data are referred to the stability axes, which are a system of axes having their origin at the center of moments shown in figure 1 and in which the Z-axis is in the plane of symmetry and perpendicular to the relative wind, the X-axis is in the plane of symmetry and perpendicular to the Z-axis, and the Y-axis is perpendicular to the plane of symmetry. The positive directions of the stability axes are shown in figure 3.

The coefficients and symbols are defined as follows:

C_L lift coefficient (Lift/qS where Lift = -Z)

C_D drag coefficient (Drag/qS where Drag = -X when ψ = 0)

C_X longitudinal-force coefficient (X/qS)

C_Y	lateral-force coefficient (Y/qS)
C_l	rolling-moment coefficient (L/qSb)
C_m	pitching-moment coefficient $(M/qS\bar{c})$
C_n	yawing-moment coefficient (N/qSb)
X	force along X-axis, pounds
Y	force along Y-axis, pounds
Z	force along Z-axis, pounds
L	rolling moment, foot-pounds
M	pitching moment, foot-pounds
N	yawing moment, foot-pounds
q	free-stream dynamic pressure, pounds per square foot $\left(\frac{1}{2}\rho V^2\right)$
S	wing area (18.264 sq ft for $\frac{1}{10}$-scale model of hypothetical flying boat, fig. 2)
$\bar{c}$	mean aerodynamic chord of wing (1.377 ft for $\frac{1}{10}$-scale model of hypothetical flying boat, fig. 2)
b	wing span (13.971 ft for $\frac{1}{10}$-scale model of hypothetical flying boat, fig. 2)
V	air velocity, feet per second
ρ	mass density of air, slugs per cubic foot
α	angle of attack of hull base line, degrees except where otherwise noted
ψ	angle of yaw, degrees
$\frac{L}{b}$	length-beam ratio, where L is distance from forward perpendicular (F.P.) to sternpost and b is maximum beam (fig. 1)

R Reynolds number, based on mean aerodynamic chord of wing of $\frac{1}{10}$-scale model of hypothetical flying boat

M Mach number $\left(\frac{\text{Airspeed}}{\text{Speed of sound in air}}\right)$

$C_{D_{min}}$ minimum drag coefficient

$C_{D_{A_{min}}}$ minimum drag coefficient based on maximum cross-sectional area A of hull (Drag/qA)

$C_{D_{V_{min}}}$ minimum drag coefficient based on volume v of hull ($\text{Drag}/qv^{2/3}$)

$C_{D_{W_{min}}}$ minimum drag coefficient based on surface area W of hull (Drag/qW)

$C_{m_\alpha} = \frac{\partial C_m}{\partial \alpha}$

$C_{n_\psi} = \frac{\partial C_n}{\partial \psi}$

$C_{Y_\psi} = \frac{\partial C_Y}{\partial \psi}$

MODEL AND APPARATUS

The hulls were designed by the Langley Hydrodynamics Division. Dimensions of the hulls are given in figure 1 and offsets are given in tables I to IV.

Langley tank model 203 $\left(\frac{L}{b} = 9\right)$ was derived from a hypothetical flying boat, Langley tank model 203A, essentially similar to the Boeing XPBB-1 flying boat (fig. 2). The form and proportions of hull 203 (all Langley tank models are referred to herein as hulls because only the hulls of the models were used for the tests) are the same as those of hull 203A except that the tail extension was refaired and the depth of step at the keel was increased from 0.89 inch to 1.16 inches. The depth of step was increased to permit adequate hydrodynamic stability at the lowest length-beam ratio. Because the depth of step is to remain a constant throughout the series, it is not to be assumed that the hydrodynamic stability is similar for the several models but it may be assumed that the change in stability is not such as to make any of the hulls unsatisfactory.

Langley tank models 213, 214, and 224 were derived from model 203 by keeping constant the product of the beam and the square of the length, the depth of step at the keel, and the maximum height of the hull. The location of the wing with respect to the step and the length of the hull aft of the step (afterbody plus length of tail extension) are the same for all models. The change in over-all length due to variation of $\frac{L}{b}$ is accomplished by varying the forebody length. The volumes, surface areas, maximum cross-sectional areas, and side areas for the four hulls are compared in the following table:

Langley tank model	$\frac{L}{b}$	Volume (cu in.)	Surface area (sq in.)	Maximum cross-sectional area (sq in.)	Side area (sq in.)
213	6	14,831	4540	226	1639
203	9	12,916	4581	182	1752
214	12	11,528	4654	150	1870
224	15	10,653	4760	130	1985

The models were mounted on a wing which was designed either to span the tunnel test section vertically as shown in figure 4 (two-dimensional mounting) or to be mounted horizontally as shown in figure 5 (three-dimensional mounting). Transformation from one mounting to the other was achieved through the use of end caps and suitable cover plates. On all models, the wing was set at an angle of incidence of 4° to the base line, had a 20-inch chord, and was of the NACA 4321 airfoil section.

The hulls and wing were of laminated-wood construction and were finished with pigmented varnish.

Step fairings that extended 9 times the corresponding depth of step at the keel were made of wooden blocks for the hulls of $\frac{L}{b} = 6$ and $\frac{L}{b} = 12$. The general proportions of the fairings are shown in figure 6.

TESTS

Test Conditions

The tests were made in the Langley 300 MPH 7- by 10-foot tunnel at dynamic pressures ranging from 25 to 200 pounds per square foot, which correspond to airspeeds ranging from 100 to 290 miles per hour. Reynolds numbers, based on the mean aerodynamic chord of the wing of the hypothetical flying boat, ranged from 1.25×10^6 to 3.40×10^6. Corresponding Mach numbers ranged from 0.13 to 0.39 (fig. 7).

Corrections

Blocking corrections have been applied to the wing and wing-plus-hull data. The drag of the hull has been corrected for horizontal buoyancy effects caused by a tunnel static-pressure gradient. Angles of attack have been corrected for structural deflections caused by aerodynamic forces.

Test Procedure

The aerodynamic characteristics of the hulls were determined with the interference of the mounting wing by testing the wing alone and the wing-plus-hull combinations under the same conditions. The aerodynamic coefficients of the hull were then determined by subtraction of wing-alone coefficients from wing-plus-hull coefficients.

In order to minimize possible errors that result from transition shifting on the wing, the wing transition was fixed at the leading edge for all tests by means of roughness strips of approximately 0.008-inch-diameter carborundum particles. The particles were applied for a length of 8 percent chord of the mounting wing measured along the airfoil contour from the leading edge on both upper and lower surfaces.

The hulls, with the exception of hull 224, were tested with fixed and free transition. For the fixed-transition tests, a transition strip $\frac{1}{2}$ inch wide was located approximately 5 percent of the hull length aft of the bow. Carborundum particles of approximately 0.008-inch diameter were used for this strip also.

With the exception of hull 224 $\left(\frac{L}{b} = 15\right)$ pitch tests were made with the model mounted horizontally and vertically to obtain

data with different tunnel-wall conditions and different mountings. Hull 224 was tested at a later date than were the hulls of lower length-beam ratios and was tested only with the horizontal mounting. All yaw tests were made with the horizontal mounting.

RESULTS AND DISCUSSION

The effects of length-beam ratio on the variation of hull aerodynamic characteristics with angle of attack are presented in figures 8 and 9 and with angle of yaw in figure 10. The effects of length-beam ratio on drag and on the stability parameters C_{m_α}, C_{n_ψ}, and C_{Y_ψ} are summarized in figure 11.

Comparison of data (figs. 8 and 9) from the two-dimensional and three-dimensional mounting setups under similar test conditions shows fairly good agreement. An increase in the length-beam ratio resulted in a reduction in the drag coefficient throughout the angle-of-attack range tested. The minimum drag coefficient for most conditions occurred in the angle-of-attack range between 2° and 3°. Because of structural limitations of the mounting wing, it was necessary to limit the data obtained at the higher Reynolds number conditions to the angle-of-attack ranges shown. With transition fixed, the minimum drag coefficient for the hull of $\frac{l}{b} = 9$ was less by a value of 0.0009 (12 percent) than the minimum drag coefficient for the hull of $\frac{l}{b} = 6$ (fig. 11). Smaller reductions in minimum drag coefficient, 0.0007 and 0.0006, occurred when $\frac{l}{b}$ was extended from 9 to 12 and from 12 to 15, respectively. The over-all reduction for an extension of $\frac{l}{b}$ from 6 to 15 was 0.0022, a reduction of 29 percent. The data for the free-transition tests show the same general variation of $C_{D_{min}}$ with $\frac{l}{b}$, and the value of $C_{D_{min}}$ is about 0.0005 lower than for the fixed-transition tests throughout the range of length-beam ratio. Reference 1 indicates that the same general trend of $C_{D_{min}}$ with $\frac{l}{b}$ will probably occur for a hull without wing interference although the absolute values will differ.

The characteristic of drag reduction with increase in length-beam ratio is similar to that reported in a British paper of limited distribution by Clark and Cameron. A comparison with data from the British paper of drag coefficients (transition free) based on cross-sectional area, volume, and surface area is presented

in figure 12. Variations of the drag coefficients with $\frac{L}{b}$ generally compare favorably. It must be remembered, however, that the hulls tested by Clark and Cameron were not designed from the same hydrodynamic criterion used in the present investigation and were tested at a lower Reynolds number. The British results are, therefore, not directly comparable with the results of the present investigation but indicate the same trends. The effect of Reynolds number on $C_{D_{min}}$ as indicated herein (fig. 13) was generally small; however, some reduction did occur with Reynolds number, especially for the transition-free condition.

In order to obtain some indication of the effect of aerodynamic refinement on the variation of $C_{D_{min}}$ with length-beam ratio, the hulls of $\frac{L}{b} = 6$ and $\frac{L}{b} = 12$ were tested with step fairings as shown in figure 6. A comparison of these data (fig. 14) with those of the original step condition shows a similar reduction in drag coefficient for both length-beam ratios; thus the same general variation of $C_{D_{min}}$ with $\frac{L}{b}$ exists. The reduction in drag coefficient was approximately 13 percent for the hull of $\frac{L}{b} = 6$ and 16 percent for the hull of $\frac{L}{b} = 12$. These data agree in general with the data of the British paper in which the drag coefficient of a hull of $\frac{L}{b} = 7$ $\left(\frac{L}{b} = 5.7 \text{ as defined in the present paper}\right)$ was decreased 16 percent by the addition of a step fairing.

Increased length-beam ratio had a beneficial effect on hull longitudinal stability but caused an increase in directional instability (fig. 11). The change in longitudinal stability corresponds to a rearward aerodynamic-center shift of about $2\frac{1}{2}$ percent mean aerodynamic chord on a flying boat when $\frac{L}{b}$ was changed from 6 to 15. Calculations made from reference 2 for the hulls without wing interference gave values of C_{m_α} approximately the same as those of figure 11, which fact indicates that the geometry of the hulls probably accounted for most of the variation of C_{m_α} with $\frac{L}{b}$. Reynolds number and transition had very little effect on C_{m_α}. At an angle of attack for minimum drag of 2°, the directional instability, measured by C_{n_ψ}, was greater for $\frac{L}{b} = 15$ than for $\frac{L}{b} = 6$, the values of C_{n_ψ} being 0.0014 and 0.0009, respectively. Increasing the angle of attack to 6° resulted in a less unstable

condition; the values of C_{n_ψ} were generally reduced about 0.0002 throughout the range of length-beam ratio.

An estimate was made to determine the drag reduction with increasing length-beam ratio for the hulls fitted with vertical tails, the sizes of which were adjusted to give the same directional stability. Calculations indicate that the increase in vertical-tail size would have a small effect on the variation of drag with length-beam ratio; as a result, the drag coefficient contributed by the vertical tail would be about 0.0002 greater for $\frac{l}{b} = 15$ than that for $\frac{l}{b} = 6$. This increase in vertical-tail size would be somewhat compensated for by an allowable decrease in horizontal-tail area at the higher length-beam ratios provided that sufficient horizontal-tail area were available for trim. The decrease in horizontal-tail area with $\frac{l}{b}$, however, would probably be less than the increase in vertical-tail area.

The parameter C_{Y_ψ} was slightly more positive at the higher length-beam ratios. Increasing the angle of attack from 2° to 6° had a negligible effect on C_{Y_ψ}. These variations of the parameters C_{Y_ψ} and C_{n_ψ} with $\frac{l}{b}$ probably result from the increase of hull length and side area ahead of the center of moment at the higher value of $\frac{l}{b}$ as shown in figure 1. For convenience the stability parameters for each value of $\frac{l}{b}$ are presented in table V. In order to compare the results of these tests with the results of investigations made of other hulls and fuselages, the parameters K_f, $\partial C_{n_f}'/\partial \psi'$, and $\partial C_n/\partial \beta$, as given in references 3, 4, and 5, respectively, are included in the table. The parameter K_f is a fuselage moment factor, in the form of $\partial C_m/\partial \alpha$, based on hull beam and length where α is in radians. The yawing-moment coefficient C_{n_f}' in $\partial C_{n_f}'/\partial \psi'$ is based on volume and is given about a reference axis 0.3 of the hull length from the nose. The parameter $\partial C_n/\partial \beta$ is based on hull side area and length for which the yawing moment is also given about a reference axis 0.3 of the hull length from the nose and β is given in radians.

Instability as given by the parameters $\partial C_{n_f}'/\partial\psi'$ and $\partial C_n/\partial\beta$ generally agreed closely with the hull values given in references 4 and 5. The increase of $\partial C_{n_f}'/\partial\psi'$ with $\frac{L}{b}$ can be attributed to the reduced numerical values of volume used in determining the coefficient at the higher length-beam ratios as well as the generally destabilizing effect of increasing $\frac{L}{b}$.

Tuft studies of the forebody bottom and step part of model 203 $\left(\frac{L}{b} = 9\right)$ are presented in figures 15 and 16, respectively.

CONCLUSIONS

The results of wind-tunnel tests of a family of hulls - in the presence of a wing - having length-beam ratios of 6, 9, 12, and 15, a constant product of the beam and the square of the length, a constant height, and the same depth of step at the keel indicated the following conclusions:

1. With transition fixed a reduction in minimum drag coefficient of 0.0022 (29 percent) occurred when length-beam ratio was extended from 6 to 15.

2 Minimum drag for all hulls tested generally occurred in the range of angle of attack from 2° to 3°.

3. Increasing length-beam ratio from 6 to 15 caused an increase in hull longitudinal stability by an amount corresponding to a rearward aerodynamic-center shift of about $2\frac{1}{2}$ percent mean aerodynamic chord on a flying boat.

4. Increasing length-beam ratio from 6 to 15 increased the hull directional instability by increasing the variation of yawing-moment coefficient with angle of yaw from a value of 0.0009 to a value of 0.0014 at an angle of attack of 2°.

5. Incorporating a hull step fairing, which extended longitudinally about 9 times the depth of the step at the keel, resulted in a reduction up to 16 percent in minimum drag coefficient.

Langley Memorial Aeronautical Laboratory
National Advisory Committee for Aeronautics
Langley Field, Va., December 12, 1946

REFERENCES

1. Jacobs, Eastman N., and Ward, Kenneth E.: Interference of Wing and Fuselage from Tests of 209 Combinations in the N.A.C.A. Variable-Density Tunnel. NACA Rep. No. 540, 1935.

2. Multhopp, H.: Aerodynamics of the Fuselage. NACA TM No. 1036, 1942.

3. Gilruth, R. R., and White, M. D.: Analysis and Prediction of Longitudinal Stability of Airplanes. NACA Rep. No. 711, 1941.

4. Pass, H. R.: Analysis of Wind-Tunnel Data on Directional Stability and Control. NACA TN No. 775, 1940.

5. Imlay, Frederick H.: The Estimation of the Rate of Change of Yawing Moment with Sideslip. NACA TN No. 636, 1938.

TABLE I

OFFSETS FOR LANGLEY TANK MODEL 213 $\left(\frac{L}{D} = 6\right)$

[All dimensions are in inches]

Station	Distance to F.P.	Keel above base line	Chine above base line	Half beam at chine	Radius and half maximum beam	Height of hull at center line	Line of centers above base line	Angle of chine flare (deg)	Forebody bottom, heights above base line								
									Buttocks								
									0.66	1.31	1.97	2.62	3.28	3.93	4.59	5.24	5.90
F.P.	0	10.30	10.92	0	0.	10.92											
1/2	1.86	5.49	9.17	3.01	3.01	14.29	11.28	10	6.79	8.11	8.96	9.20					
1	3.71	3.76	7.63	4.01	4.01	15.72	11.71	10	4.76	5.78	6.80	7.43	7.71	7.64			
2	7.42	1.83	5.45	5.06	5.06	17.36	12.30	10	2.58	3.31	4.06	4.69	5.17	5.46	5.51		
3	11.14	.80	4.00	5.66	5.66	18.41	12.85	10	1.34	1.90	2.45	3.02	3.49	3.81	4.01	4.05	
4	14.85	.27	3.01	6.04	6.04	19.12	13.08	10	.69	1.12	1.55	1.99	2.39	2.72	2.97	3.09	3.04
5	18.56	.04	2.36	6.28	6.28	19.60	13.32	10	.37	.71	1.04	1.35	1.69	1.98	2.22	2.37	2.41
6	22.27	0	1.98	6.41	6.41	19.88	13.47	5	.25	.52	.77	1.02	1.28	1.54	1.74	1.91	1.99
7	25.98	0	1.83	6.45	6.45	19.99	13.54	0	.24	.47	.72	.96	1.21	1.43	1.61	1.74	1.83
8	29.70	0	1.83	6.455	6.455	20.00	13.55	0	.24	.47	.72	.96	1.21	1.43	1.61	1.74	1.83
9	33.41	0	1.83	6.455	6.455	20.00	13.55	0	.24	.47	.72	.96	1.21	1.43	1.61	1.74	1.83
10	37.12	0	1.83	6.455	6.455	20.00	13.55	0	.24	.47	.72	.96	1.21	1.43	1.61	1.74	1.83
11	40.83	0	1.83	6.455	6.455	20.00	13.55	0	.24	.47	.72	.96	1.21	1.43	1.61	1.74	1.83
12F	44.58	0	1.83	6.455	6.455	20.00	13.55	0	.24	.47	.72	.96	1.21	1.43	1.61	1.74	1.83
12A	44.58	1.16	3.51	6.455	6.455	20.00	13.55										
13	48.26	1.51	3.83	6.36	6.43	20.00	13.57										
14	51.97	1.86	4.08	6.09	6.39	20.00	13.61										
15	55.68	2.21	4.28	5.70	6.30	20.00	13.70										
16	59.39	2.56	4.47	5.24	6.17	20.00	13.83										
17	63.10	2.91	4.57	4.57	6.01	20.00	13.99										
18	66.82	3.26	4.63	3.76	5.81	20.00	14.19										
19	70.53	3.61	4.59	2.70	5.57	20.00	14.43										
20	74.24	3.96	4.47	1.39	5.28	20.00	14.72										
S.P.	77.45	4.27	4.27	0													
21	77.95	4.69			4.95	20.00	15.05										
22	81.66	7.47			4.58	20.00	15.42										
23	85.37	9.70			4.16	20.00	15.84										
24	89.08	11.50			3.70	20.00	16.30										
25	92.79	12.90			3.22	20.00	16.78										
26	96.50	14.18			2.70	20.00	17.30										
27	100.22	15.47			2.15	20.00	17.85										
28	103.93	16.74			1.55	20.00	18.45										
29	107.64	18.02			.93	20.00	19.07										
A.P.	110.19	18.90			.51	20.00	19.49										

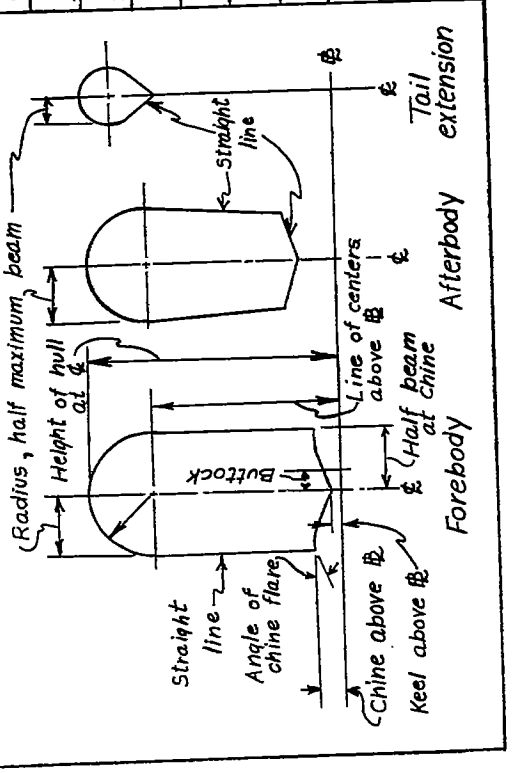

TABLE II

OFFSETS FOR LANGLEY TANK MODEL 203 $\left(\frac{L}{D} = 9\right)$

[All dimensions are in inches]

Station	Distance to P.P.	Keel above base line	Chine above base line	Half beam at chine	Radius and half maximum beam	Height of hull at center line	Line of centers above base line	Angle of chine flare (deg)	Forebody bottom, heights above base line								
									Buttocks								
									$\frac{1}{2}$	1	$1\frac{1}{2}$	2	$2\frac{1}{2}$	3	$3\frac{1}{2}$	4	$4\frac{1}{2}$
F.P.	0	10.30	10.30	0	0	11.00	11.00										
1/2	2.13	5.49	8.30	2.30	2.30	14.29	11.98	10	6.48	7.49	8.14	8.32					
1	4.25	3.76	6.71	3.06	3.06	15.72	12.66	10	4.52	5.30	6.09	6.56	6.77	6.72			
2	8.50	1.83	4.59	3.86	3.86	17.36	13.50	10	2.40	2.96	3.53	4.01	4.38	4.60	4.64		
3	12.75	.80	3.24	4.32	4.32	18.41	14.08	10	1.21	1.64	2.06	2.49	2.85	3.10	3.25	3.28	
4	17.00	.27	2.36	4.61	4.61	19.12	14.52	10	.59	.92	1.25	1.58	1.89	2.14	2.33	2.42	2.38
5	21.25	.04	1.81	4.79	4.79	19.60	14.81	10	.29	.55	.80	1.04	1.30	1.52	1.70	1.82	1.85
6	25.50	0	1.51	4.89	4.89	19.88	14.99	5	.19	.40	.59	.78	.98	1.18	1.33	1.46	1.52
7	29.75	0	1.40	4.92	4.92	19.99	15.07	0	.18	.36	.55	.73	.92	1.09	1.23	1.33	1.40
8	34.00	0	1.40	4.925	4.925	20.00	15.08	0	.18	.36	.55	.73	.92	1.09	1.23	1.33	1.40
9	38.25	0	1.40	4.925	4.925	20.00	15.08	0	.18	.36	.55	.73	.92	1.09	1.23	1.33	1.40
10	42.50	0	1.40	4.925	4.925	20.00	15.08	0	.18	.36	.55	.73	.92	1.09	1.23	1.33	1.40
11	46.75	0	1.40	4.925	4.925	20.00	15.08	0	.18	.36	.55	.73	.92	1.09	1.23	1.33	1.40
12F	51.04	0	1.40	4.925	4.925	20.00	15.08	0	.18	.36	.55	.73	.92	1.09	1.23	1.33	1.40
12A	51.04	1.16	2.95	4.925	4.925	20.00	15.08										
13	55.25	1.56	3.32	4.85	4.91	20.00	15.09										
14	59.50	1.96	3.65	4.65	4.86	20.00	15.14										
15	63.75	2.36	3.94	4.35	4.77	20.00	15.23										
16	68.00	2.76	4.22	4.00	4.65	20.00	15.33										
17	72.25	3.16	4.43	3.49	4.48	20.00	15.52										
18	76.50	3.56	4.61	2.87	4.28	20.00	15.73										
19	80.75	3.97	4.72	2.06	4.03	20.00	15.97										
20	85.00	4.37	4.75	1.06	3.73	20.00	16.27										
S.P.	88.68	4.72	4.72	0													
21	89.25	5.28			3.40	20.00	16.60										
22	93.50	8.71			3.02	20.00	16.98										
23	97.75	11.43			2.61	20.00	17.39										
24	102.00	13.61			2.16	20.00	17.84										
25	106.25	15.31			1.69	20.00	18.31										
26	110.50	16.78			1.17	20.00	18.83										
27	114.75	18.25			.63	20.00	19.37										
A.P.	116.65	18.90			.39	20.00	19.61										

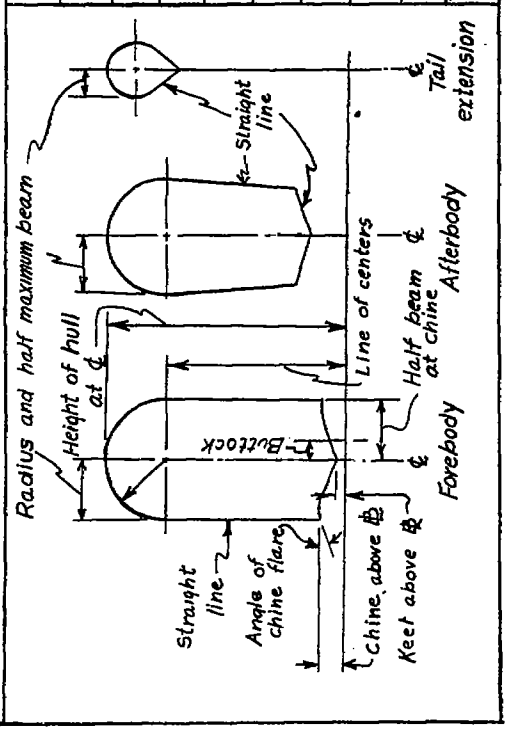

TABLE III

OFFSETS FOR LANGLEY TANK MODEL 214 $\left(\frac{L}{b} = 12\right)$

[All dimensions are in inches]

Station	Distance to P.P.	Keel above base line	Chine above base line	Half beam at chine	Radius and half maximum beam	Height of hull at center line	Line of centers above base line	Angle of chine flare (deg)	Forebody bottom, heights above base line								
									Buttocks								
									0.41	0.83	1.24	1.65	2.06	2.48	2.89	3.30	3.72
F.P.	0	10.15	10.15	0	0	11.14											
1/2	2.34	5.49	7.81	1.90	1.90	14.29	12.39	10	6.31	7.14	7.68	7.83					
1	4.68	3.76	6.20	2.53	2.53	15.72	13.19	10	4.39	5.03	5.67	6.07	6.24	6.20			
2	9.35	1.83	4.11	3.19	3.19	17.36	14.17	10	2.30	2.76	3.23	3.63	3.94	4.12	4.15		
3	14.03	.80	2.81	3.57	3.57	18.41	14.84	10	1.14	1.49	1.84	2.20	2.49	2.70	2.82	2.85	
4	18.71	.27	2.00	3.81	3.81	19.12	15.31	10	.53	.81	1.08	1.35	1.61	1.81	1.97	2.05	2.01
5	23.38	.04	1.50	3.96	3.96	19.60	15.64	10	.25	.46	.67	.86	1.08	1.26	1.41	1.51	1.53
6	28.06	0	1.25	4.04	4.04	19.88	15.84	5	.16	.33	.49	.64	.81	.97	1.10	1.21	1.26
7	32.74	0	1.16	4.06	4.06	19.99	15.93	0	.15	.30	.45	.60	.76	.90	1.02	1.10	1.16
8	37.41	0	1.16	4.065	4.065	20.00	15.93	0	.15	.30	.45	.60	.76	.90	1.02	1.10	1.16
9	42.09	0	1.16	4.065	4.065	20.00	15.93	0	.15	.30	.45	.60	.76	.90	1.02	1.10	1.16
10	46.77	0	1.16	4.065	4.065	20.00	15.93	0	.15	.30	.45	.60	.76	.90	1.02	1.10	1.16
11	51.44	0	1.16	4.065	4.065	20.00	15.93	0	.15	.30	.45	.60	.76	.90	1.02	1.10	1.16
12F	56.17	0	1.16	4.065	4.065	20.00	15.93	0	.15	.30	.45	.60	.76	.90	1.02	1.10	1.16
12A	56.17	1.16	2.64	4.065	4.065	20.00	15.93										
13	60.80	1.60	3.06	4.00	4.05	20.00	15.95										
14	65.47	2.04	3.44	3.84	4.01	20.00	15.99										
15	70.15	2.48	3.79	3.59	3.93	20.00	16.07										
16	74.83	2.92	4.12	3.30	3.80	20.00	16.20										
17	79.50	3.37	4.42	2.88	3.62	20.00	16.30										
18	84.18	3.81	4.67	2.37	3.41	20.00	16.59										
19	88.86	4.25	4.87	1.70	3.17	20.00	16.83										
20	93.53	4.69	5.01	.88	2.87	20.00	17.13										
S.P.	97.59	5.08	5.08	0													
21	98.21	5.74			2.53	20.00	17.47										
22	102.89	9.90			2.16	20.00	17.84										
23	107.56	13.05			1.75	20.00	18.25										
24	112.24	15.45			1.31	20.00	18.69										
25	116.92	17.23			.84	20.00	19.16										
26	121.59	18.83			.34	20.00	19.66										
A.P.	121.78	18.90			.32	20.00	19.68										

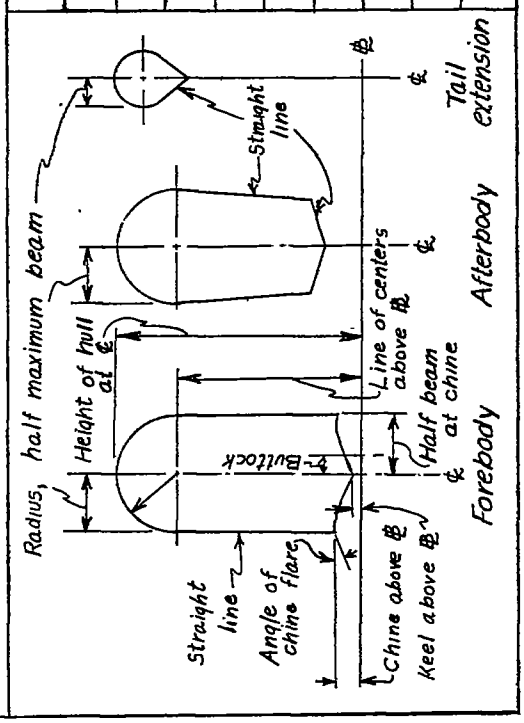

TABLE IV

OFFSETS FOR LANGLEY TANK MODEL 224 $\left(\frac{L}{D} = 15\right)$

[All dimensions are in inches]

Station	Distance to F.P.	Keel above base line	Chine above base line	Half beam at chine	Radius and half maximum beam	Height of hull at center line	Line of centers above base line	Angle of chine flare (deg)	Forebody bottom, heights above base line — Buttocks								
									0.36	0.71	1.07	1.42	1.78	2.13	2.49	2.85	3.20
F.P.	0	10.30	10.30	0	0	11.00	11.00										
½	2.52	5.49	7.49	1.64	1.64	14.29	12.65	10	6.19	6.91	7.38	7.50					
1	5.04	3.76	5.86	2.18	2.18	15.72	13.54	10	4.30	4.86	5.42	5.75	5.90	5.87			
2	10.08	1.83	3.79	2.75	2.75	17.36	14.61	10	2.24	2.63	3.04	3.38	3.64	3.80	3.83		
3	15.12	.80	2.54	3.07	3.07	18.41	15.34	10	1.09	1.40	1.70	2.00	2.26	2.44	2.54	2.57	
4	20.15	.27	1.76	3.28	3.28	19.12	15.84	10	.50	.73	.97	1.20	1.42	1.60	1.74	1.80	1.77
5	25.19	.04	1.30	3.41	3.41	19.60	16.19	10	.22	.40	.58	.75	.94	1.09	1.22	1.31	1.33
6	30.23	0	1.07	3.48	3.48	19.88	16.40	5	.14	.28	.42	.56	.70	.84	.95	1.04	1.08
7	35.27	0	1.00	3.50	3.50	19.99	16.49	0	.13	.26	.39	.52	.65	.78	.88	.95	1.00
8	40.31	0	1.00	3.505	3.505	20.00	16.49	0	.13	.26	.39	.52	.65	.78	.88	.95	1.00
9	45.34	0	1.00	3.505	3.505	20.00	16.49	0	.13	.26	.39	.52	.65	.78	.88	.95	1.00
10	50.38	0	1.00	3.505	3.505	20.00	16.49	0	.13	.26	.39	.52	.65	.78	.88	.95	1.00
11	55.42	0	1.00	3.505	3.505	20.00	16.49	0	.13	.26	.39	.52	.65	.78	.88	.95	1.00
12F	60.51	0	1.00	3.505	3.505	20.00	16.49	0	.13	.26	.39	.52	.65	.78	.88	.95	1.00
12A	60.51	1.16	2.43	3.505	3.505	20.00	16.49										
13	65.50	1.63	2.89	3.45	3.48	20.00	16.52										
14	70.54	2.11	3.31	3.31	3.44	20.00	16.56										
15	75.58	2.58	3.71	3.10	3.35	20.00	16.65										
16	80.61	3.06	4.10	2.85	3.23	20.00	16.77										
17	85.65	3.54	4.44	2.48	3.07	20.00	16.93										
18	90.69	4.01	4.75	2.04	2.84	20.00	17.16										
19	95.73	4.49	5.02	1.46	2.58	20.00	17.42										
20	100.77	4.97	5.24	.75	2.29	20.00	17.71										
AP	105.13	15.38	5.38	0	2.00	20.00	18.00										
21	105.80	6.19			1.96	20.00	18.04										
22	110.84	11.17			1.59	20.00	18.41										
23	115.88	14.63			1.19	20.00	18.81										
24	120.92	17.09			.75	20.00	19.25										
25	125.96	18.84			.29	20.00	19.71										
A.P.	126.12	18.90			.28	20.00	19.72										

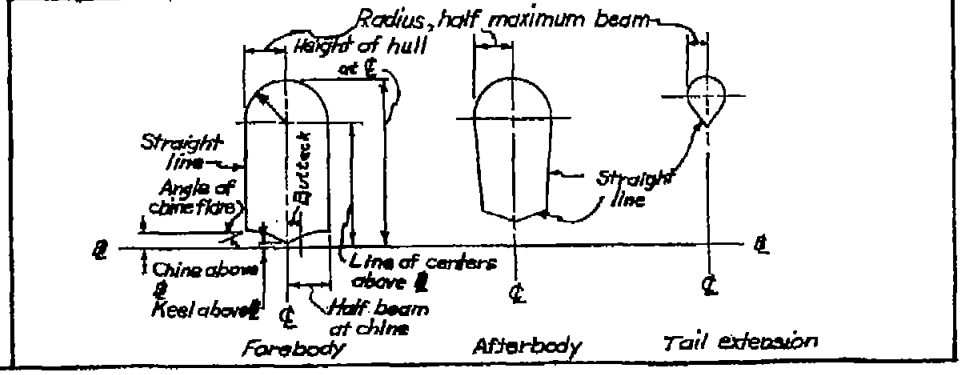

TABLE V

MINIMUM DRAG COEFFICIENTS AND STABILITY PARAMETERS FOR LANGLEY TANK MODELS 213, 203, 214, AND 224

Model	$\frac{L}{b}$	$C_{D_{min}}$	C_{m_α}	K_f	C_{Y_ψ}		C_{n_ψ}		$\partial C_n/\partial\beta$		$\partial C_{n_f}'/\partial\psi'$	
					$\alpha = 2^\circ$	$\alpha = 6^\circ$	$\alpha = 2^\circ$	$\alpha = 6^\circ$	$\alpha = 2^\circ$	$\alpha = 6^\circ$	$\alpha = 2^\circ$	$\alpha = 6^\circ$
213	6	0.0075	0.0062	0.83	0.0048	0.0048	0.0009	0.0008	-0.099	-0.081	0.021	0.017
203	9	.0066	.0050	1.10	.0051	.0050	.0012	.0010	-.100	-.088	.027	.023
214	12	.0059	.0043	1.35	.0051	.0051	.0013	.0012	-.100	-.115	.034	.040
224	15	.0053	.0038	1.56	.0051	.0051	.0014	.0013	-.101	-.126	.041	.052

NATIONAL ADVISORY
COMMITTEE FOR AERONAUTICS

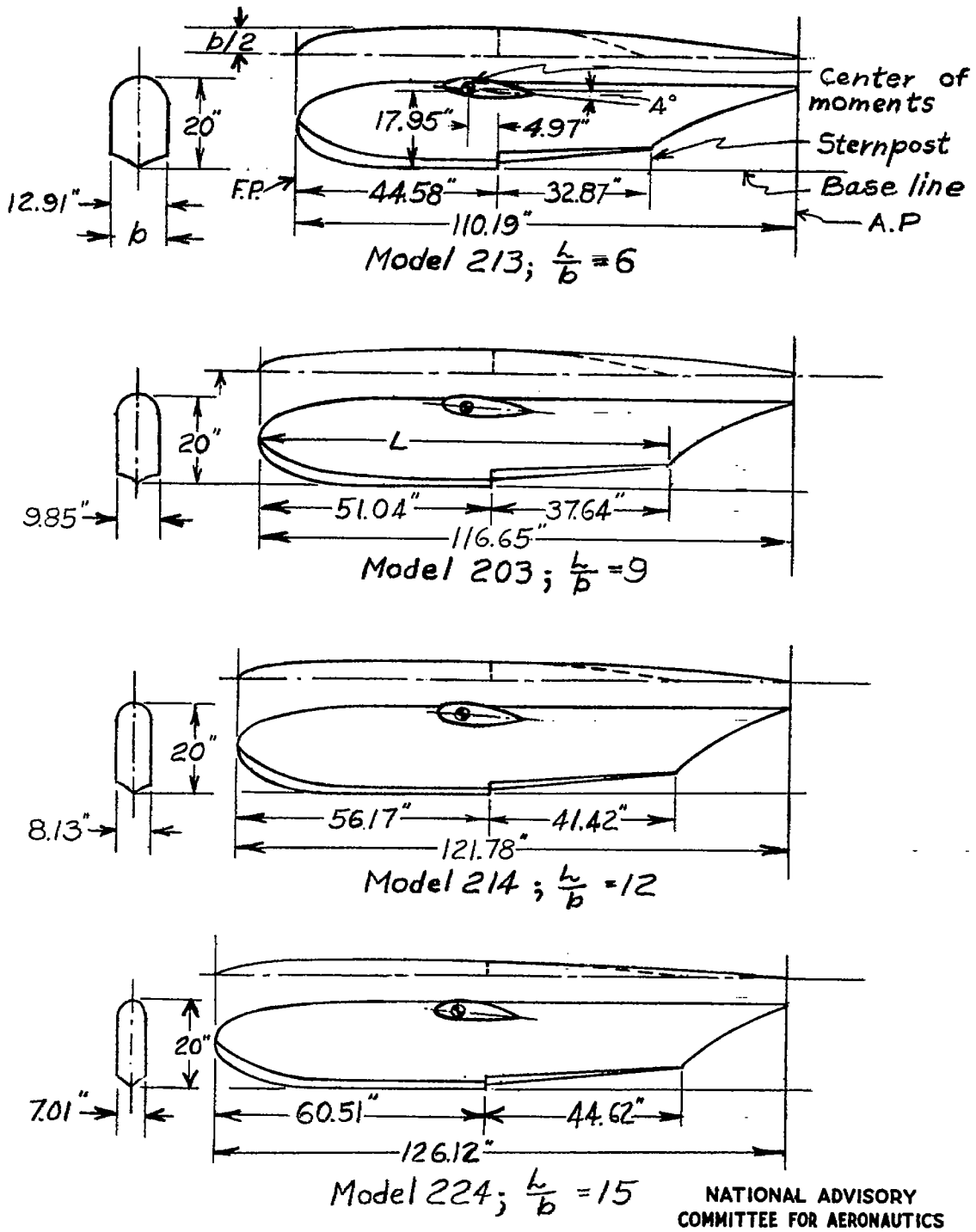

Figure 1.— Lines of Langley tank models 203, 213, 214, and 224.

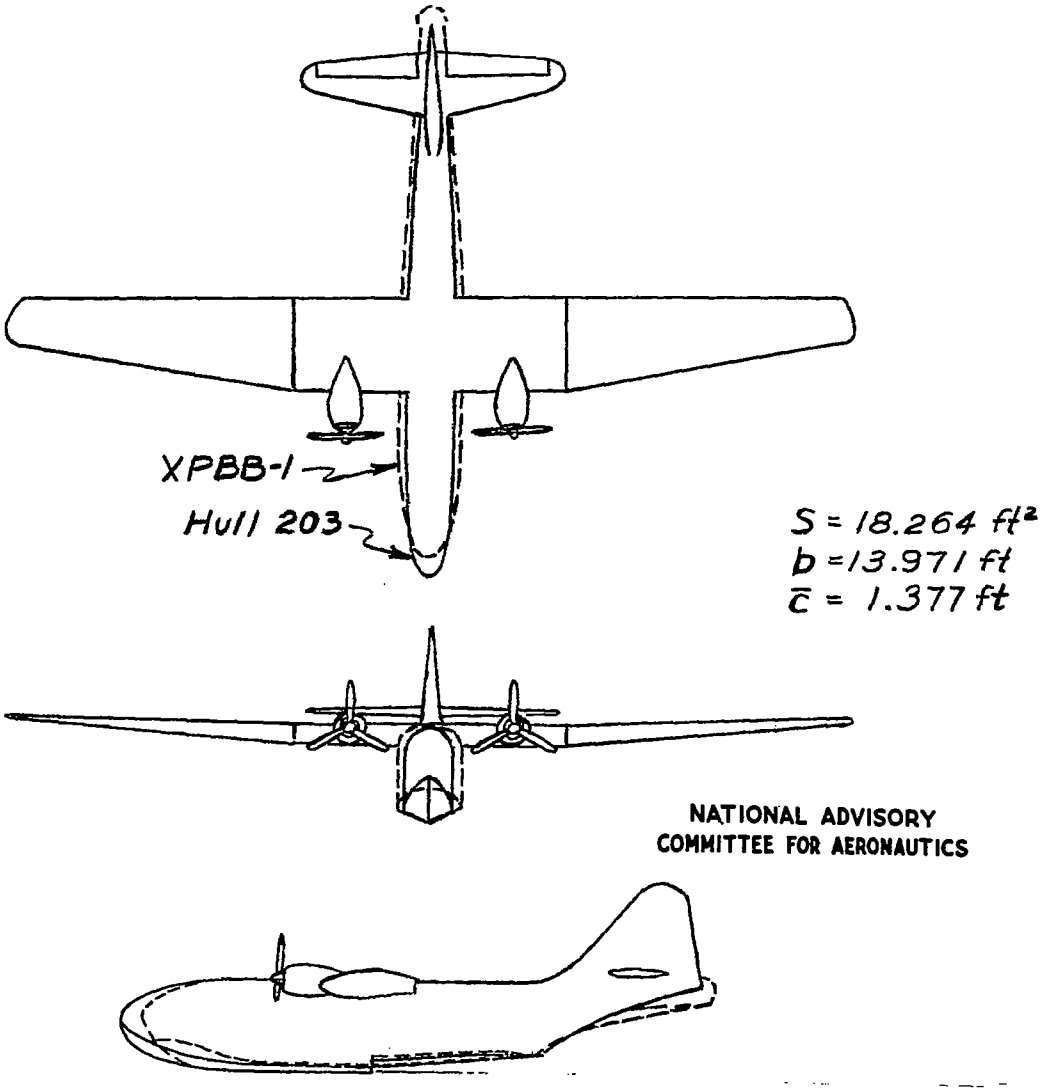

Figure 2.— Comparison of $\frac{1}{10}$-scale models of the XPBB-1 flying boat and hypothetical flying boat incorporating hull 203 $\left(\frac{L}{b} = 9\right)$.

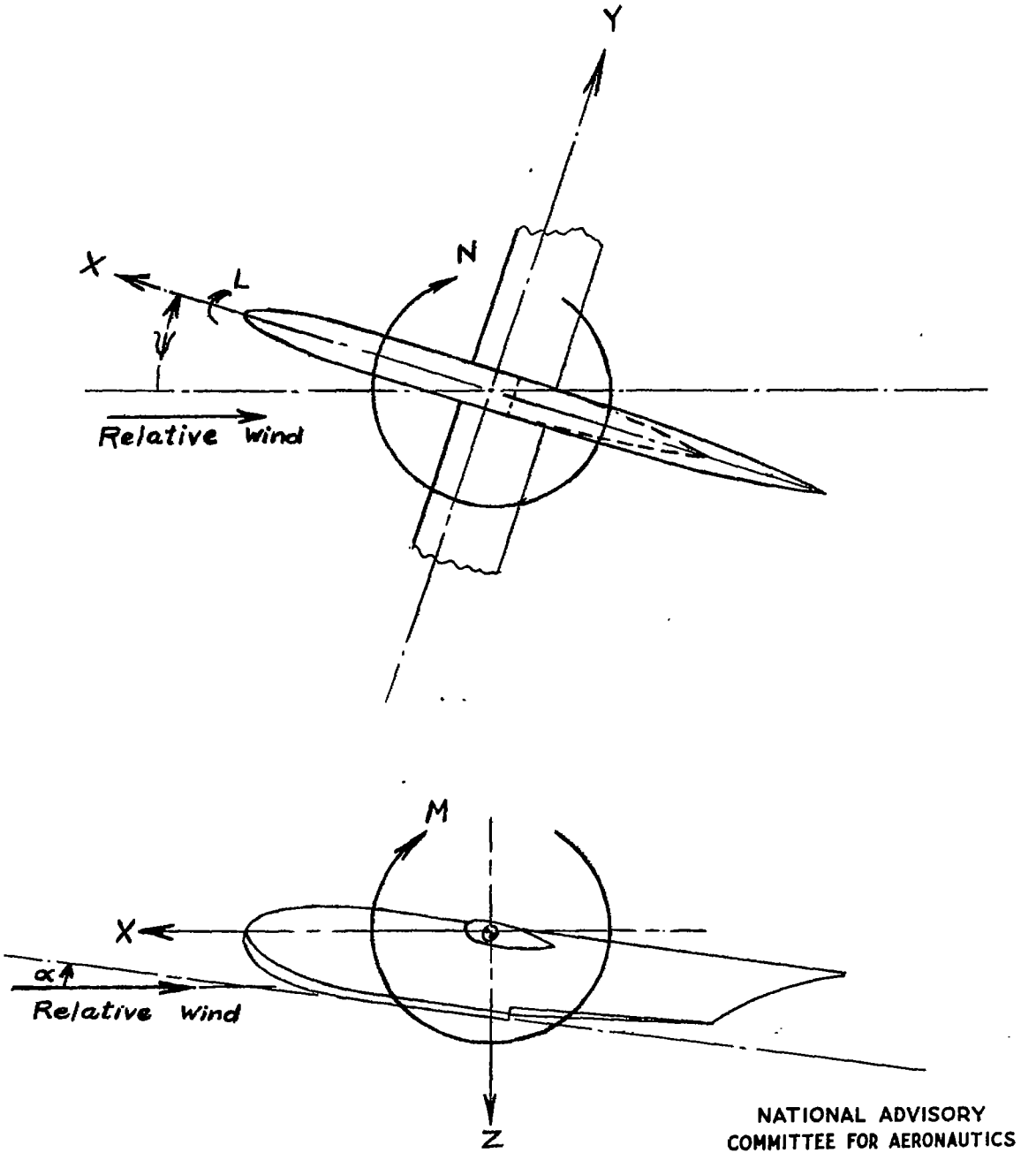

Figure 3.– System of stability axes. Positive values of forces, moments, and angles are indicated by arrows.

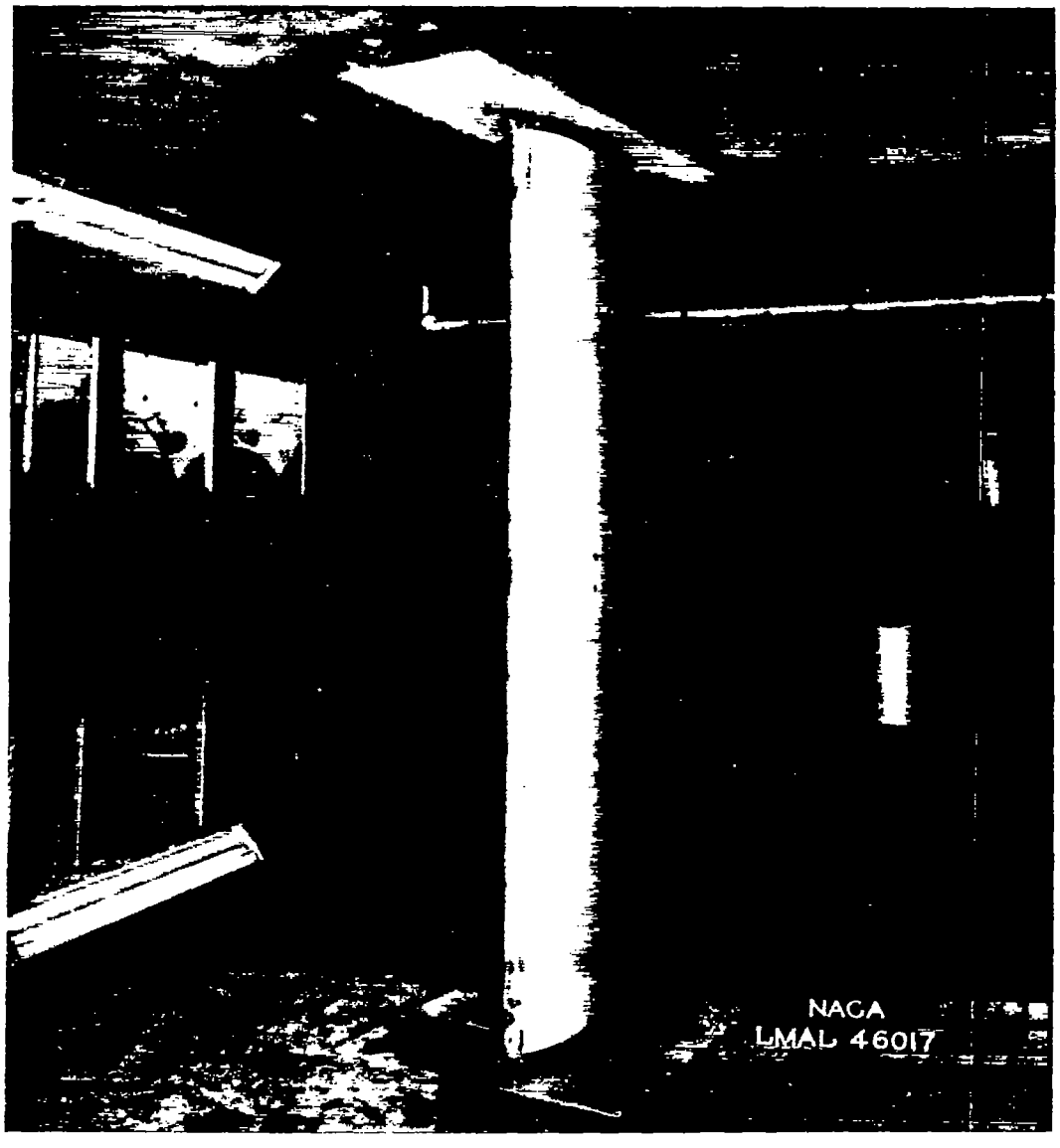

(a) Wing alone.

Figure 4.- Two-dimensional mounting of flying-boat hulls in the Langley 300 MPH 7- by 10-foot tunnel.

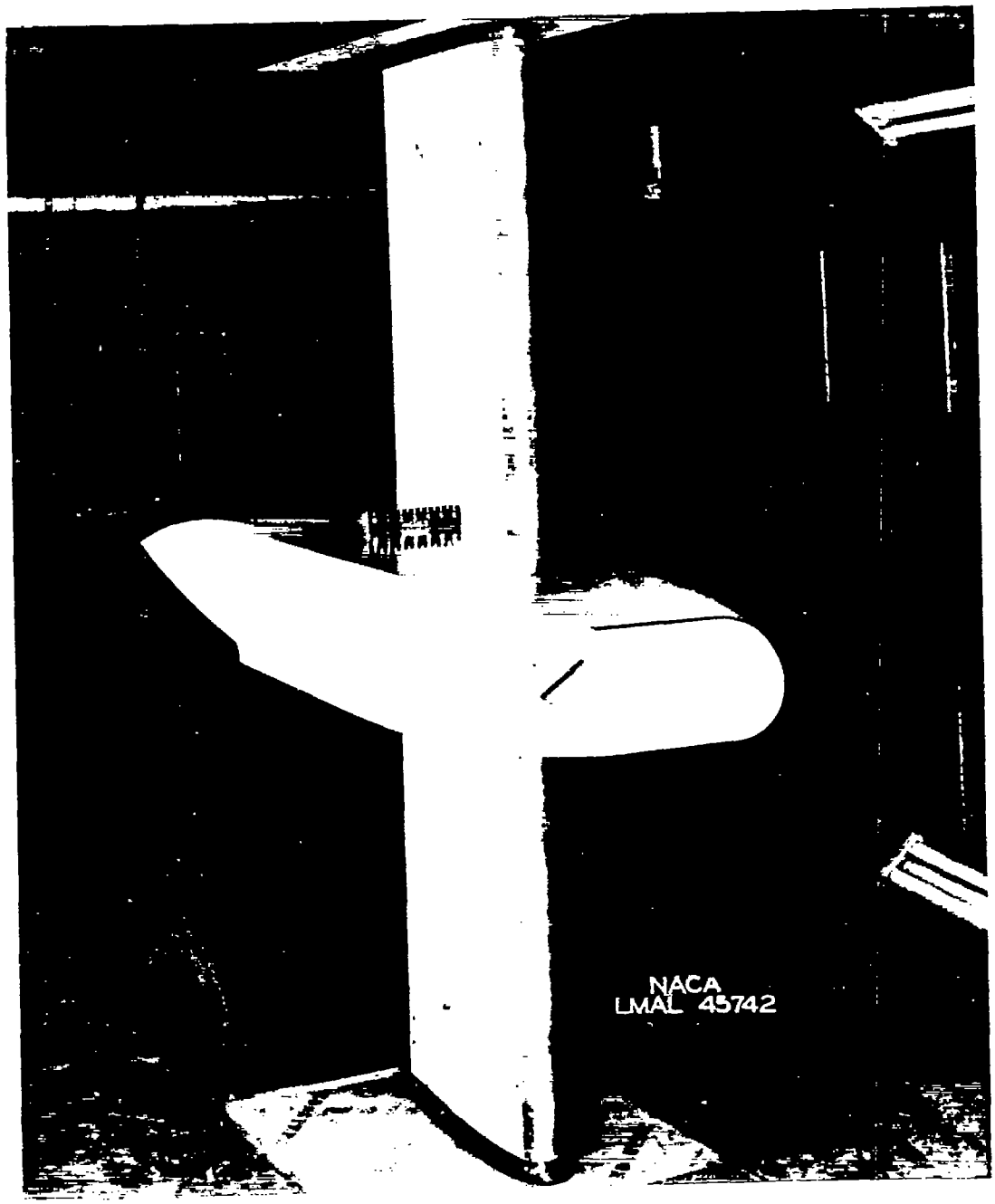

(b) Hull 203 $\left(\frac{L}{b} = 9\right)$ with wing.

Figure 4.- Concluded.

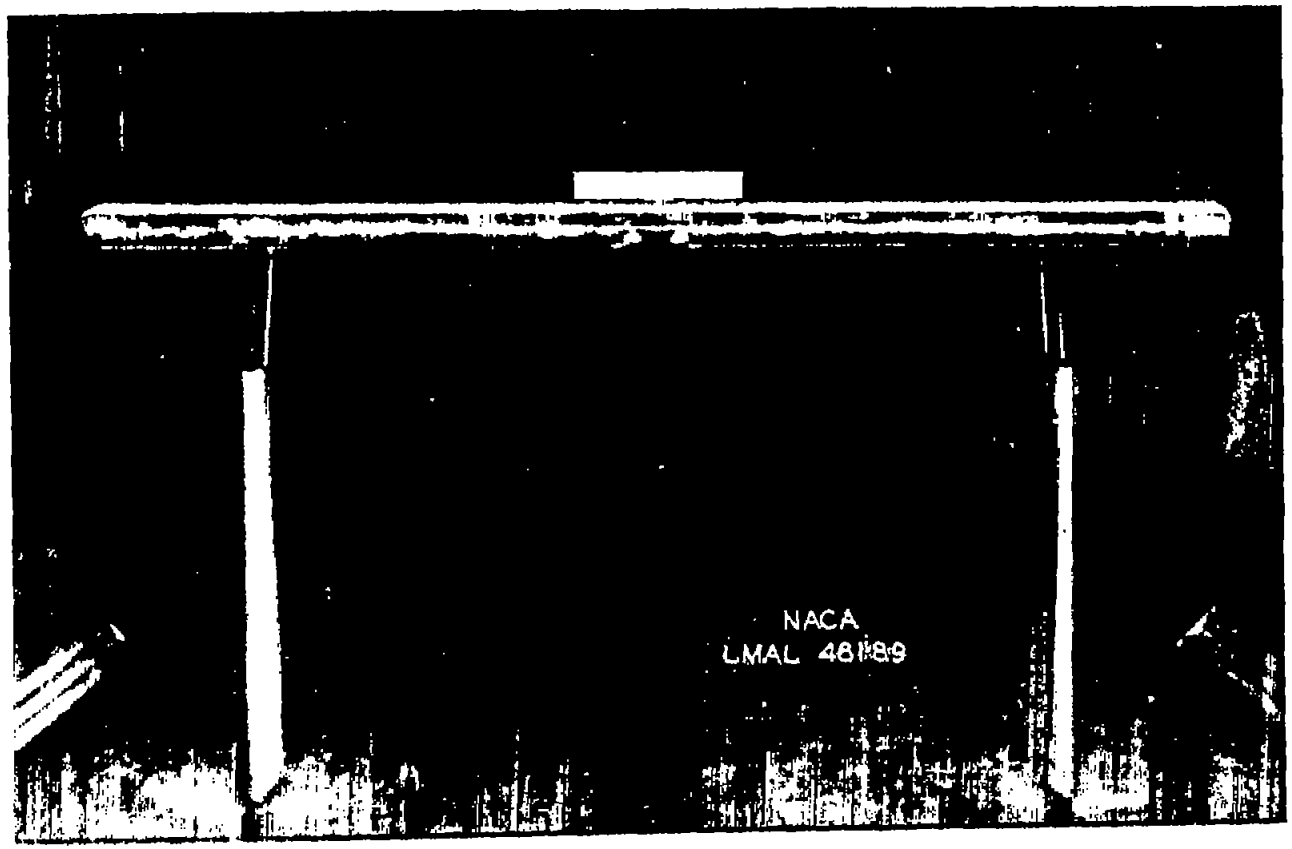

(a) Wing alone.

Figure 5.- Three-dimensional mounting of flying-boat hulls in the Langley 300 MPH 7- by 10-foot tunnel.

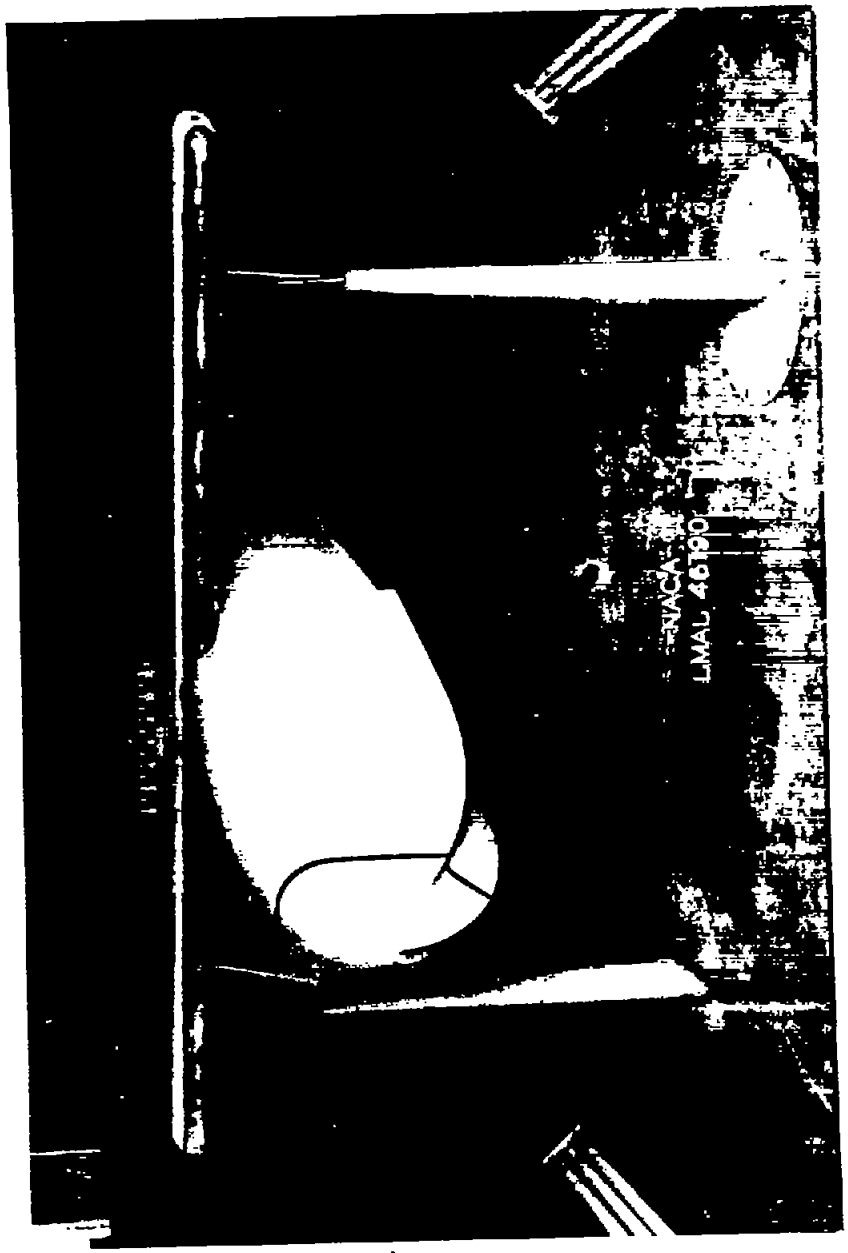

(b) Hull 203 $\left(\frac{L}{b} = 9\right)$ with wing.

Figure 5.- Concluded.

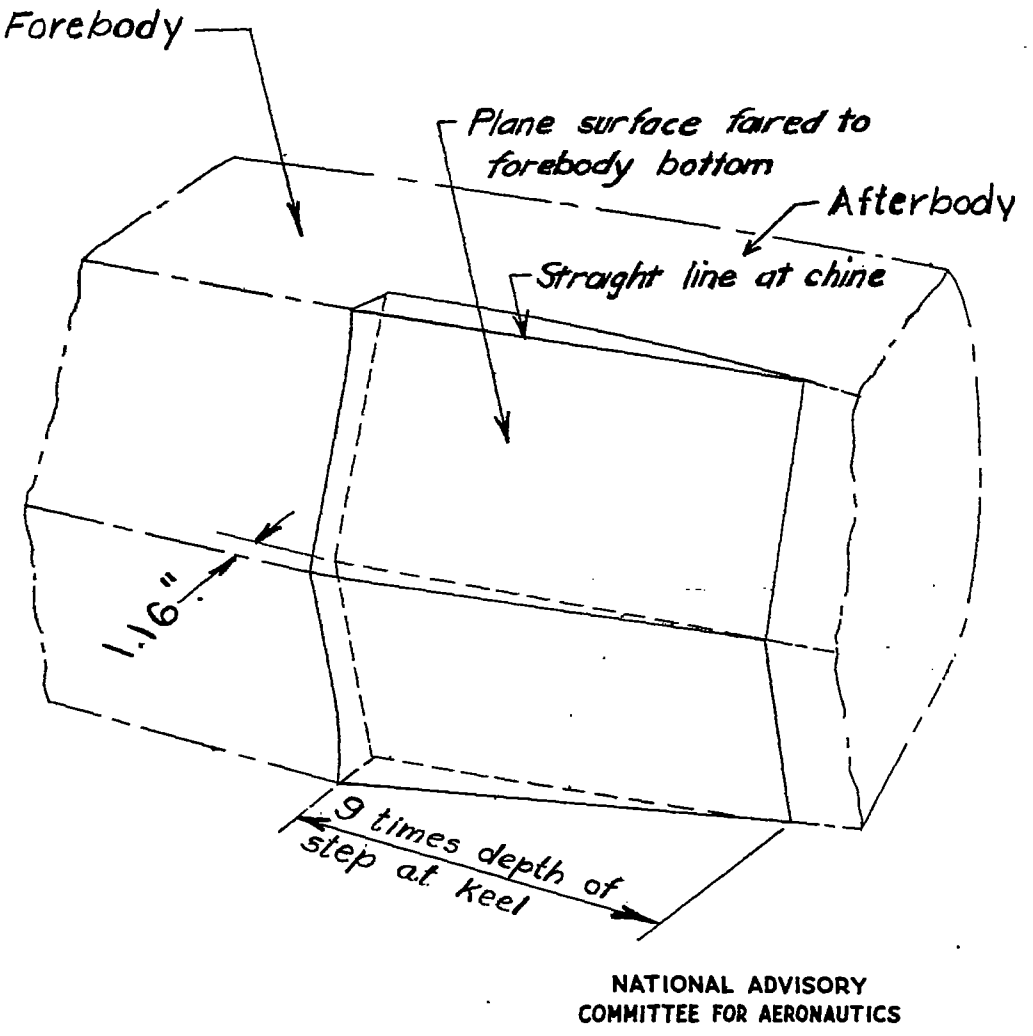

Figure 6.- General details of step fairings. Bottom view of hull.

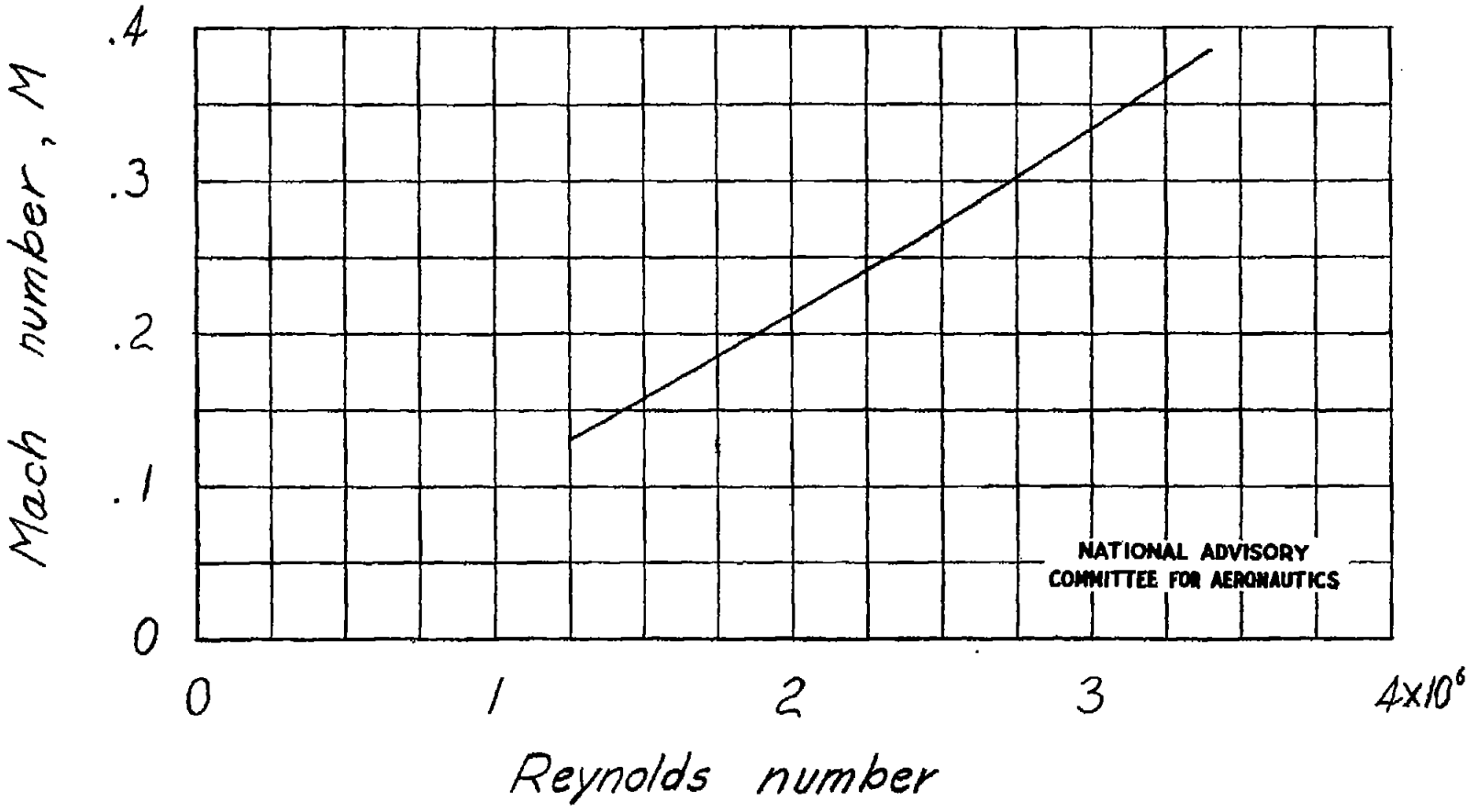

Figure 7.- Variation of Mach number with Reynolds number of the $\frac{1}{10}$-scale hulls of a hypothetical flying boat.

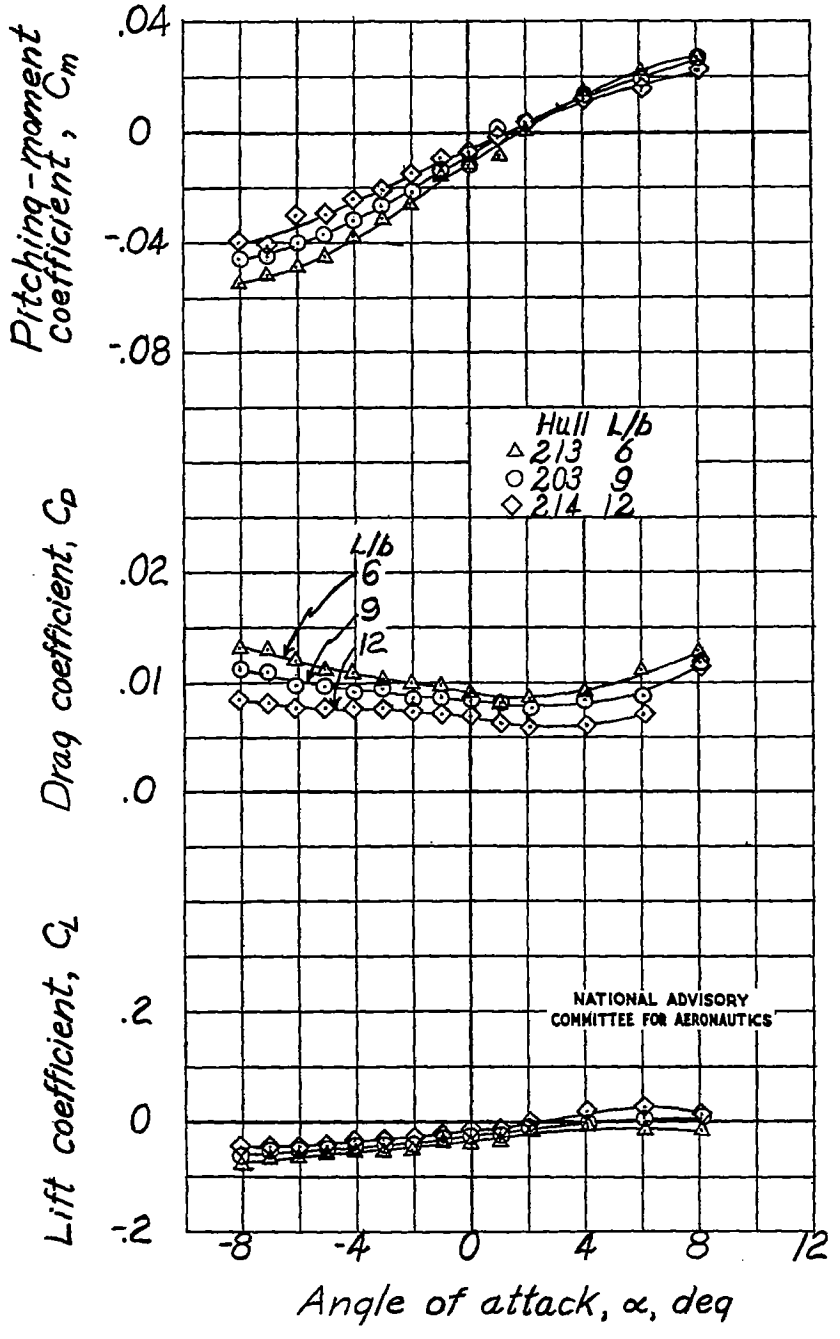

(a) R = 1,250,000; transition fixed.

Figure 8.- Effect of length-beam ratio on the aerodynamic characteristics in pitch of the $\frac{1}{10}$-scale hulls of a hypothetical flying boat. Two-dimensional mounting.

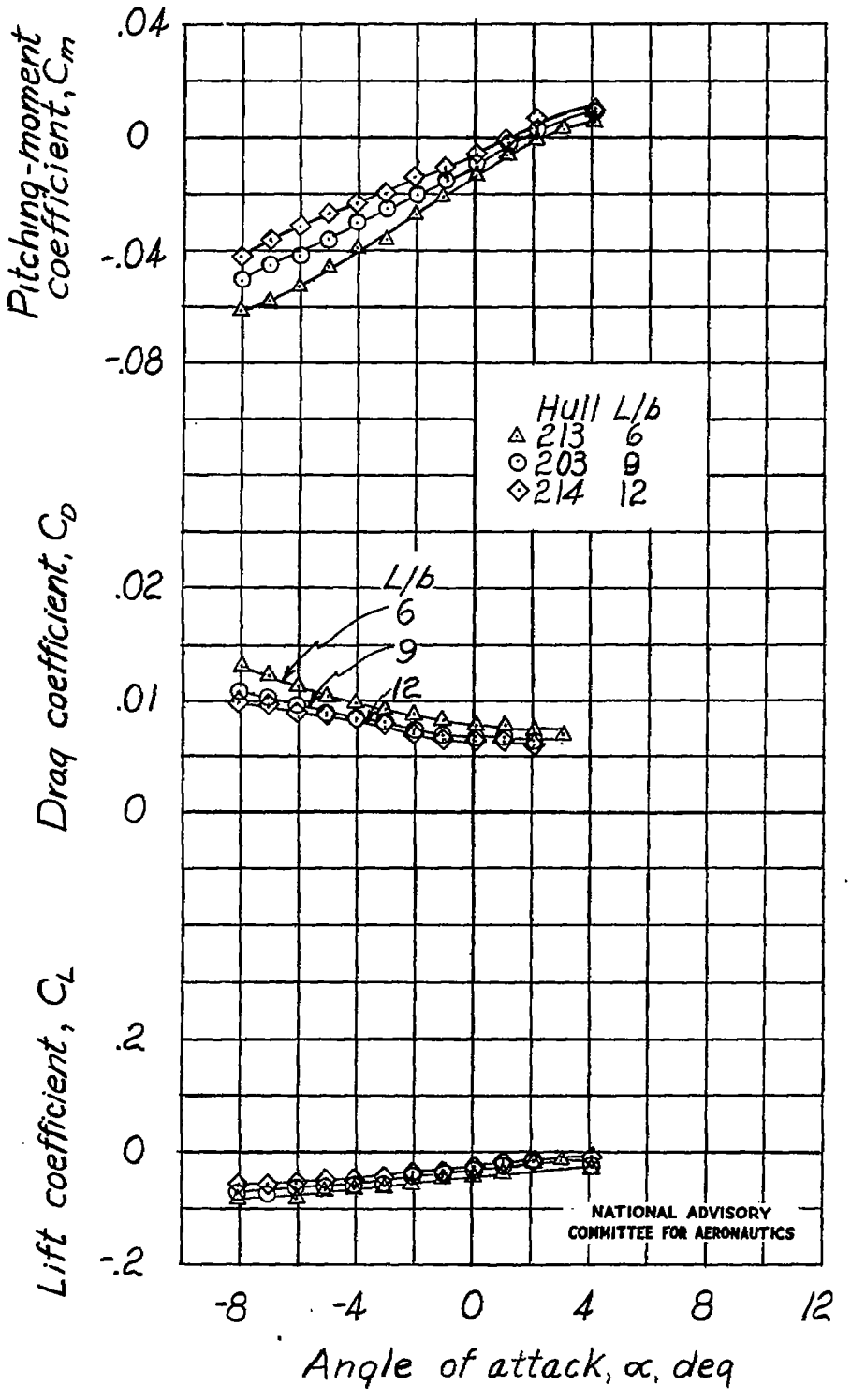

(b) R = 2,450,000; transition fixed.

Figure 8.- Continued.

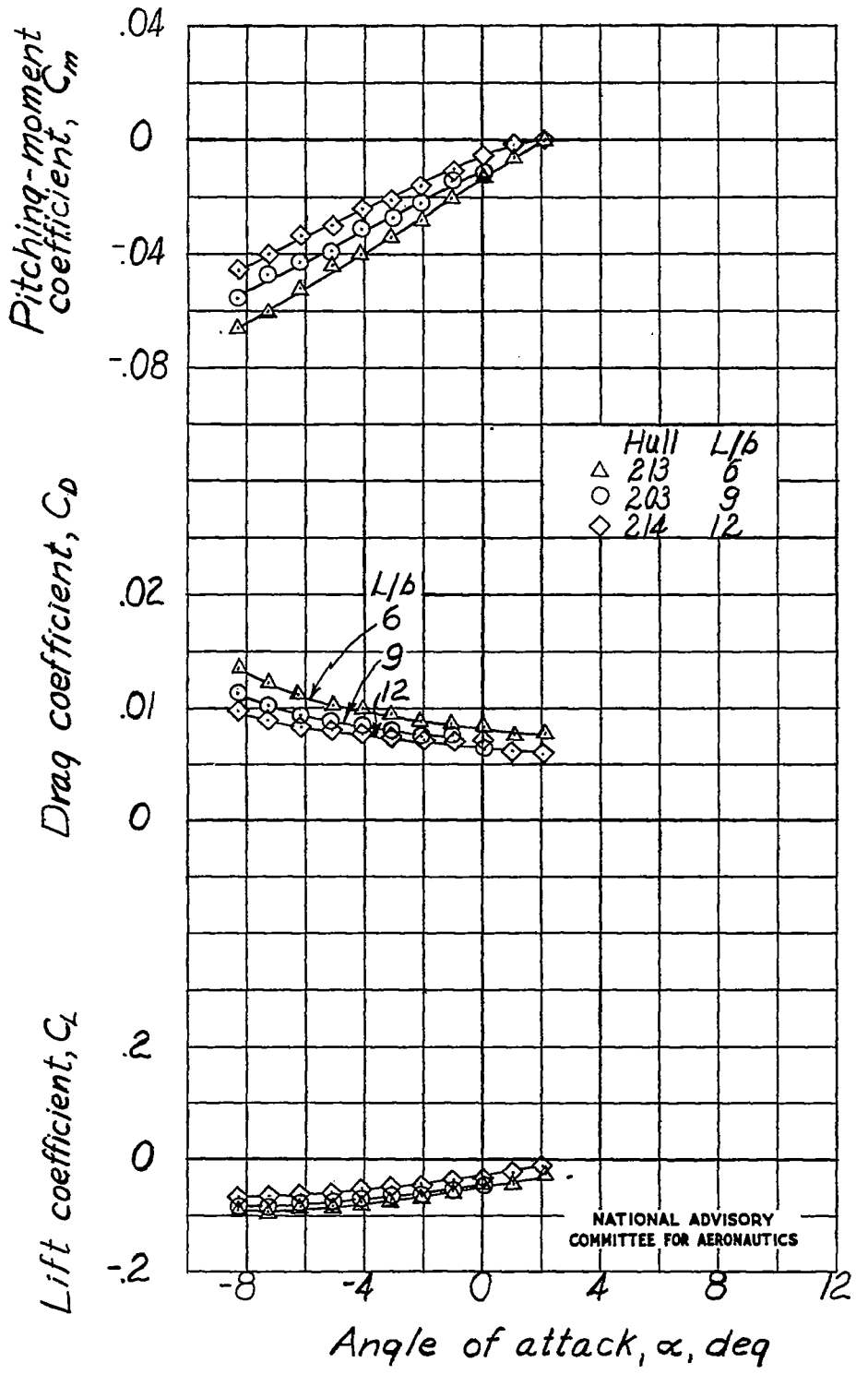

(c) R = 3,400,000; transition fixed.

Figure 8.- Continued.

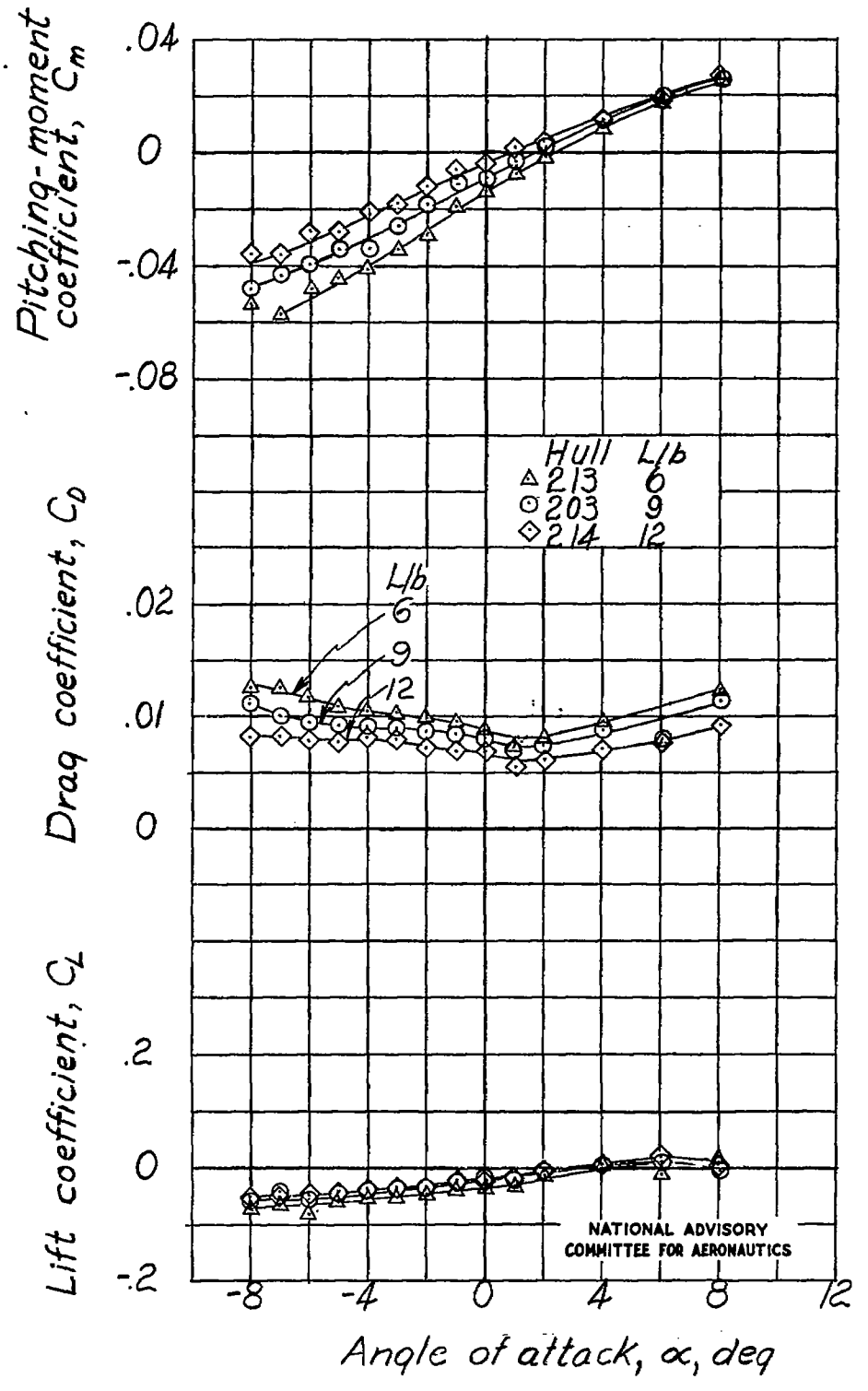

(d) R = 1,250,000; transition free.

Figure 8.- Continued.

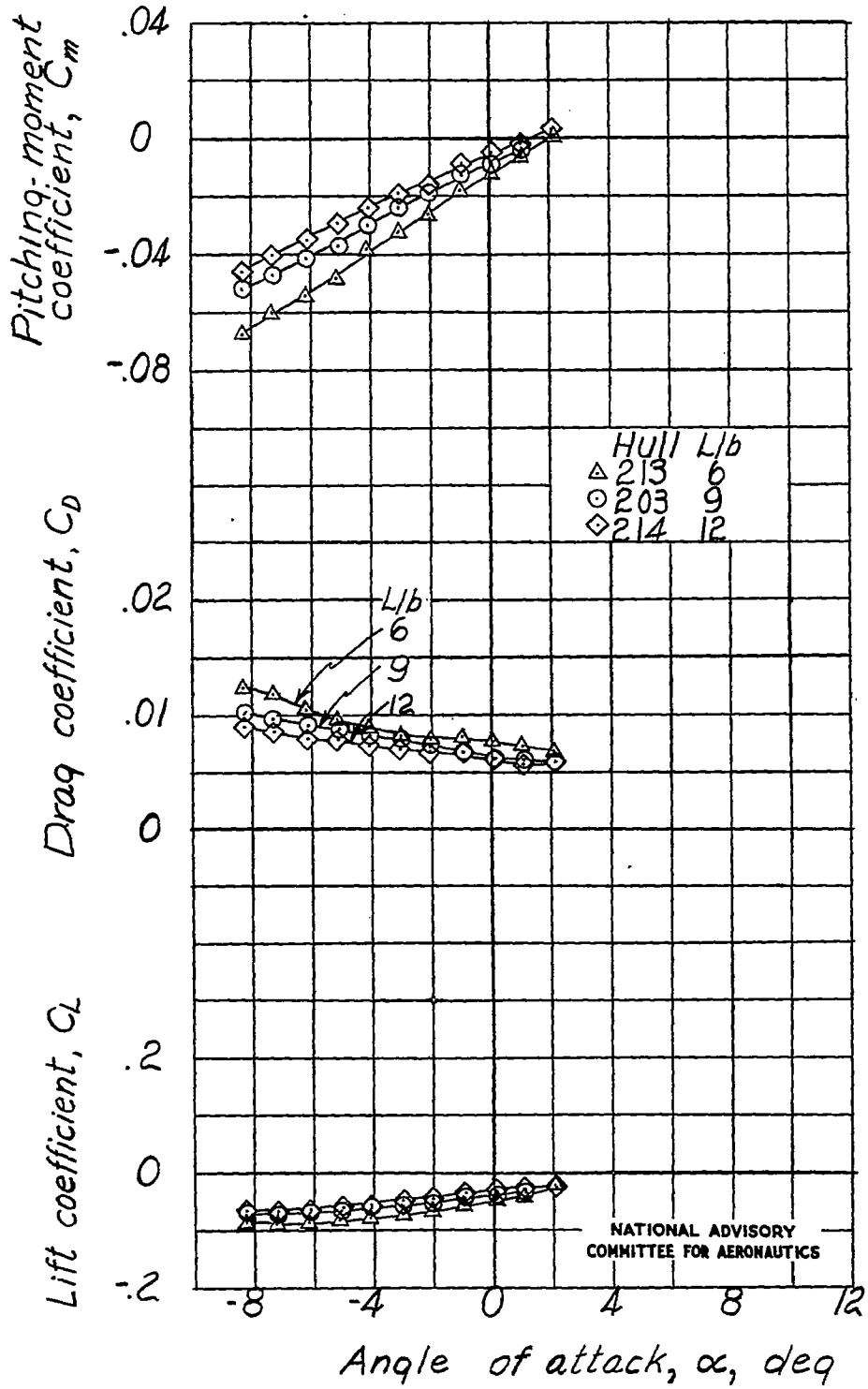

(e) R = 3,400,000; transition free.

Figure 8.- Concluded.

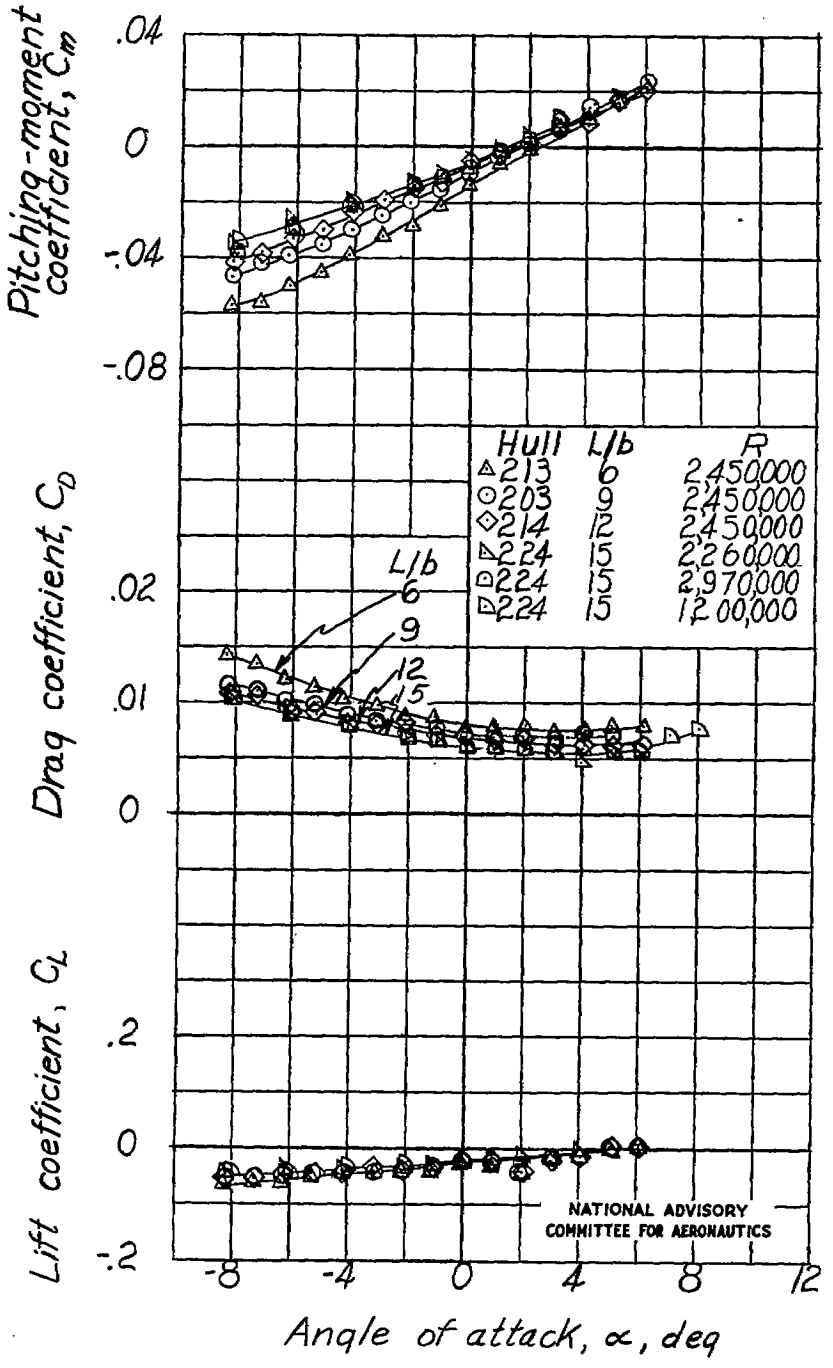

Figure 9.- Effect of length-beam ratio on the aerodynamic characteristics in pitch of the $\frac{1}{10}$-scale hulls of a hypothetical flying boat, transition fixed. Three-dimensional mounting.

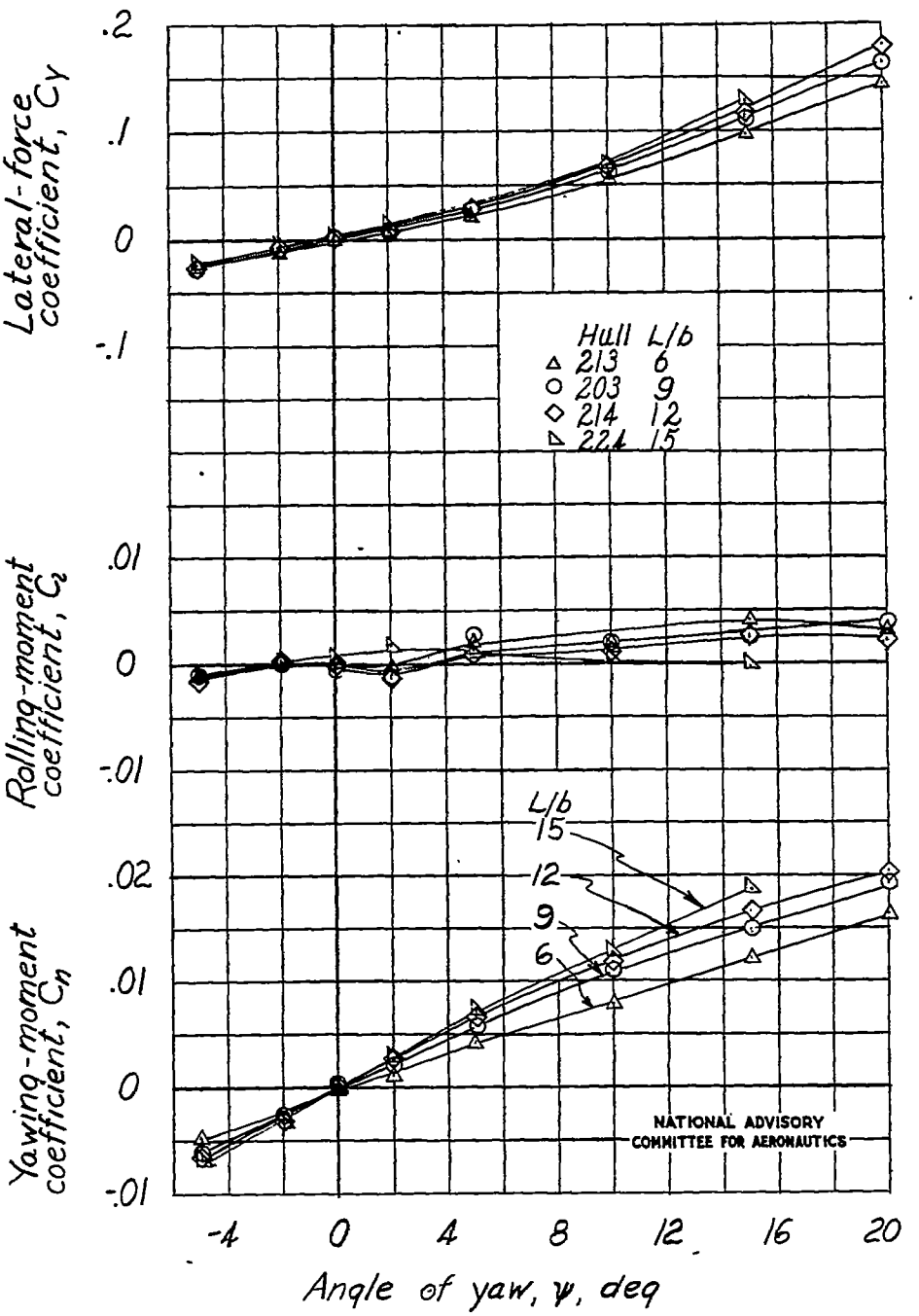

(a) $\alpha = 2^\circ$; R = 1,250,000; transition fixed.

Figure 10.- Effect of length-beam ratio on the aerodynamic characteristics in yaw of the $\frac{1}{10}$-scale hulls of a hypothetical flying boat. Three-dimensional mounting.

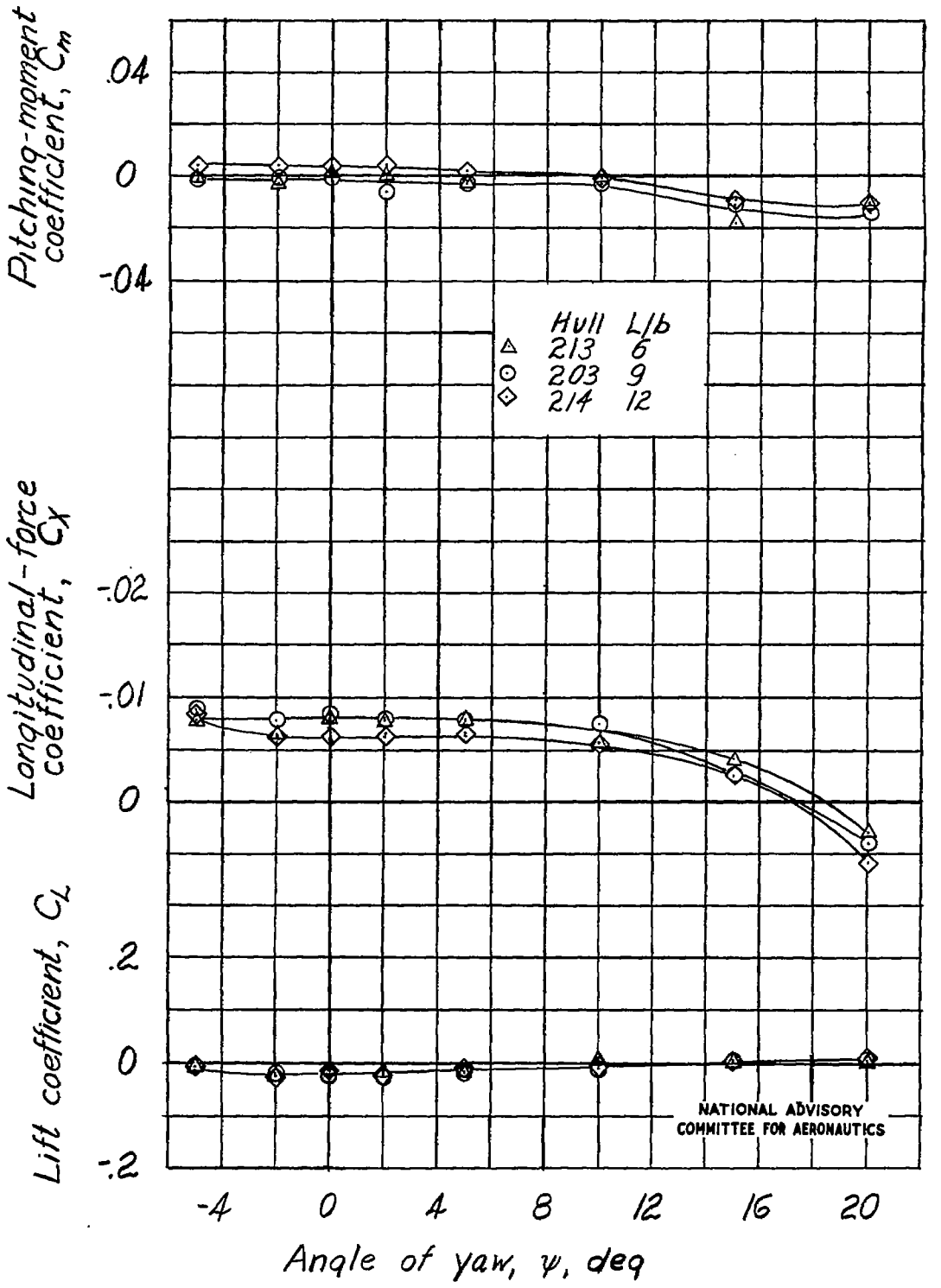

(a) Concluded.

Figure 10.- Continued.

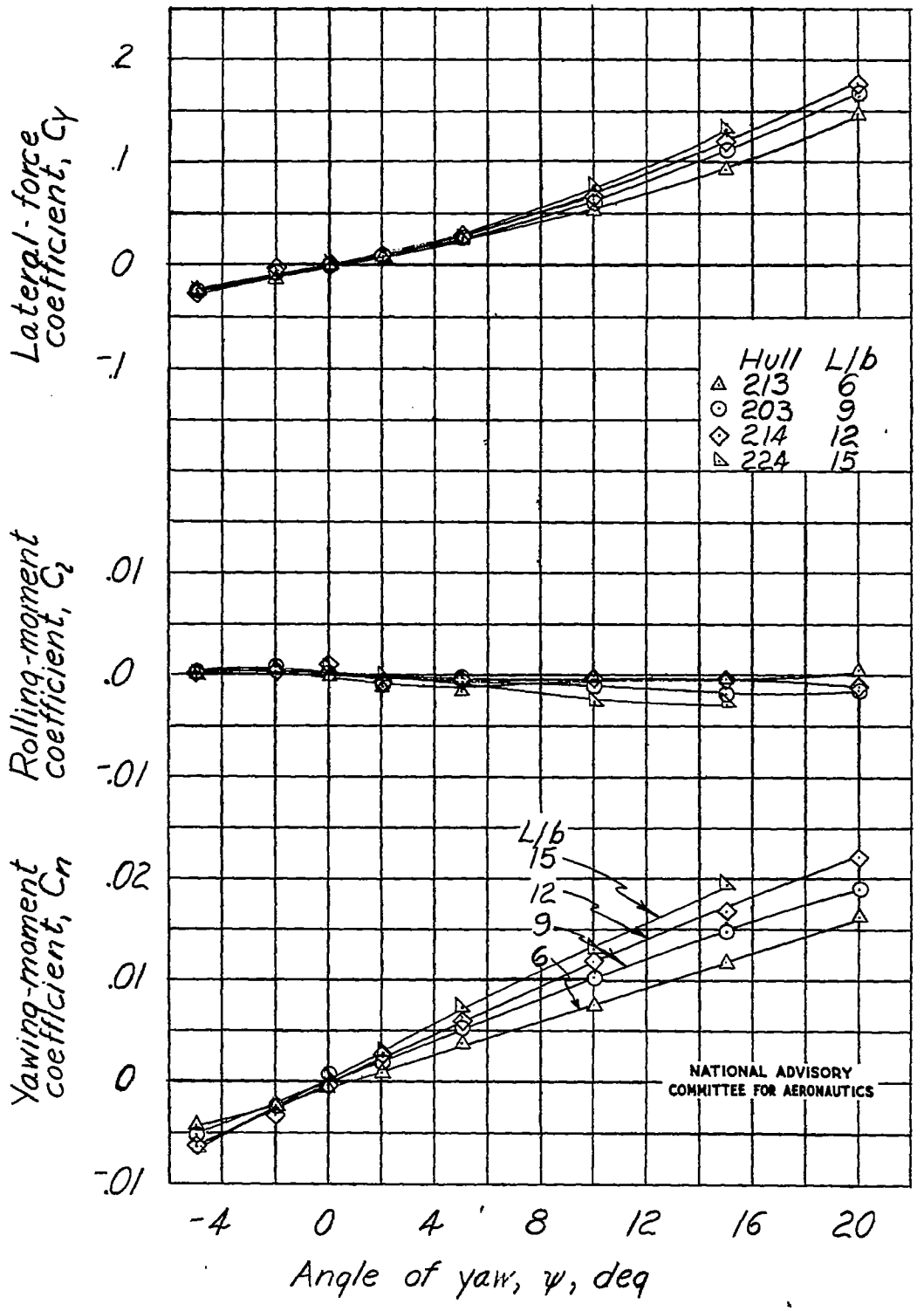

(b) $\alpha = 6^\circ$; R = 1,250,000; transition fixed.

Figure 10.- Continued.

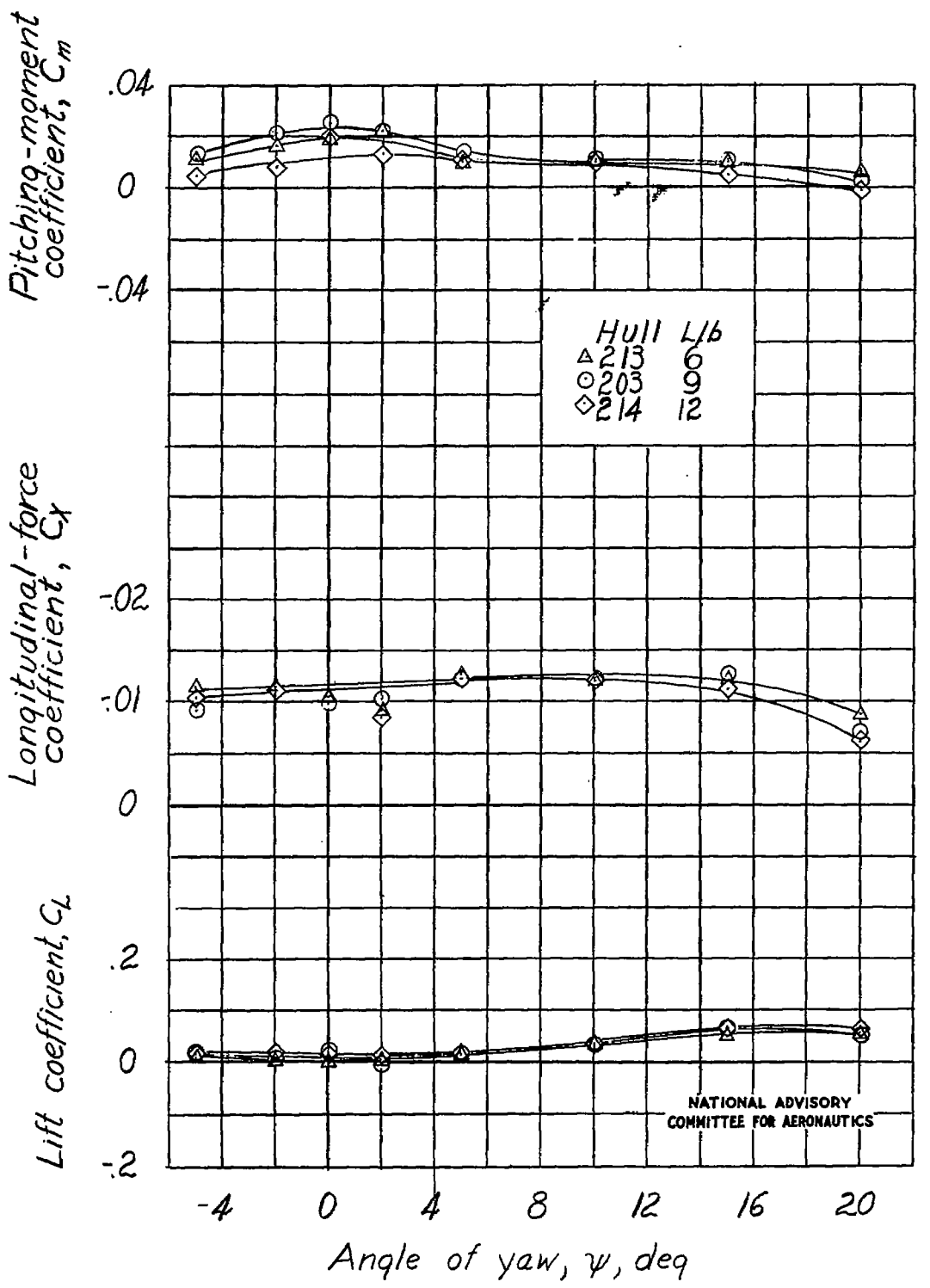

(b) Concluded.

Figure 10.- Concluded.

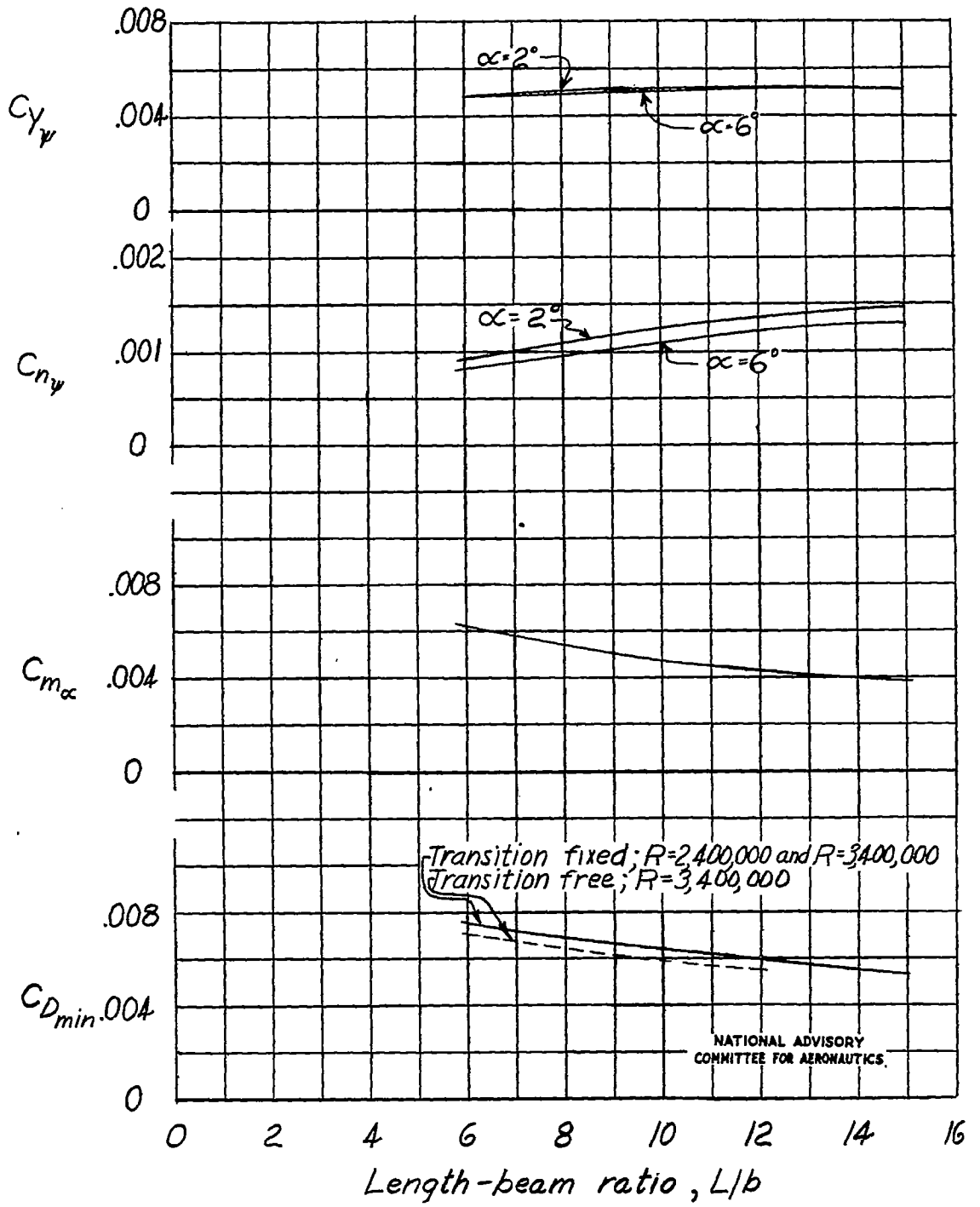

Figure 11.- Effect of length-beam ratio on $C_{D_{min}}$ and the parameters C_{m_α}, C_{n_ψ}, C_{Y_ψ} for the $\frac{1}{10}$-scale hulls of a hypothetical flying boat.

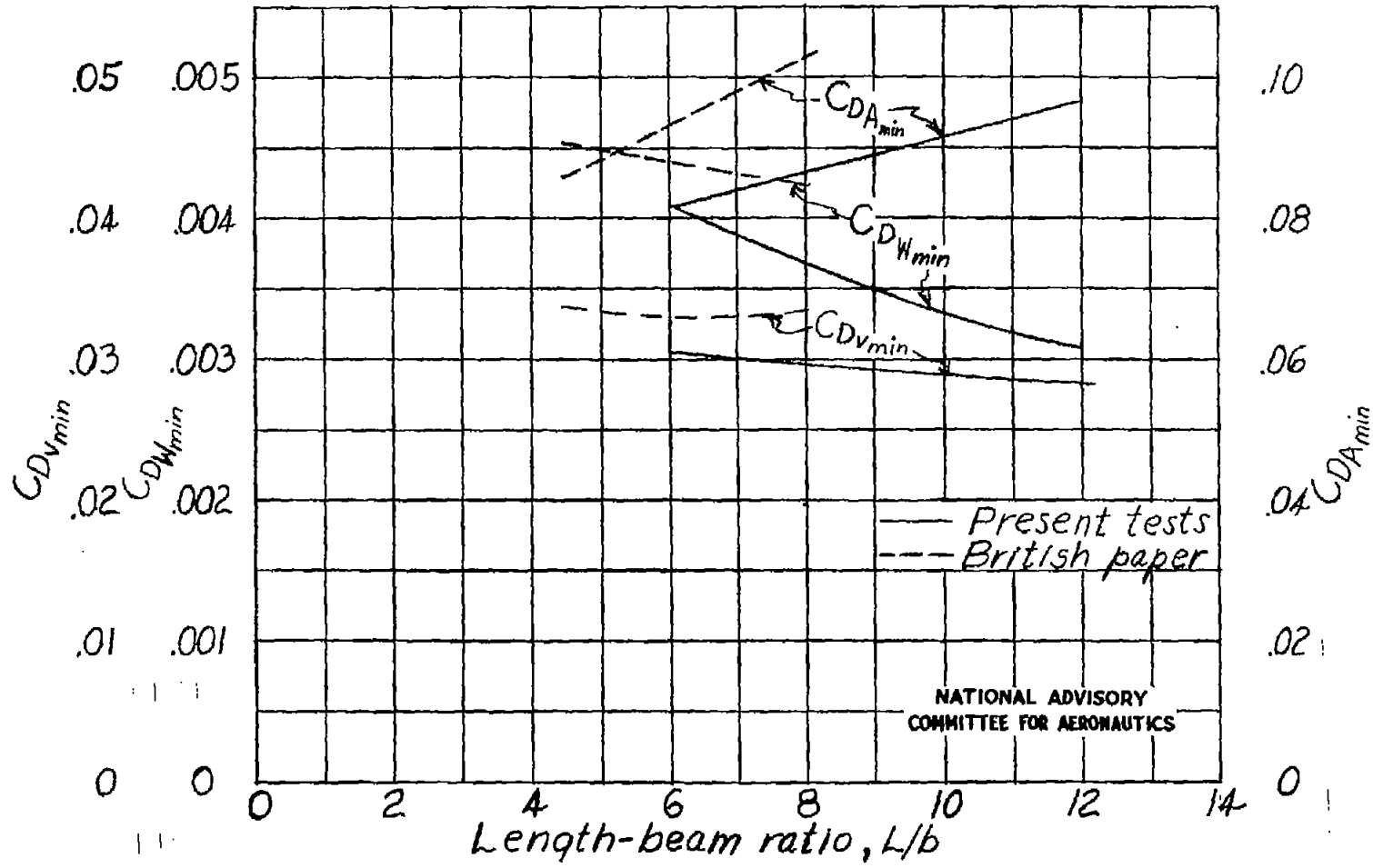

Figure 12.- Effect of length-beam ratio on the minimum drag coefficients $C_{D_{A_{min}}}$, $C_{D_{V_{min}}}$, $C_{D_{W_{min}}}$ for the $\frac{1}{10}$-scale hulls of a hypothetical flying boat and for hulls tested by the British. Transition free.

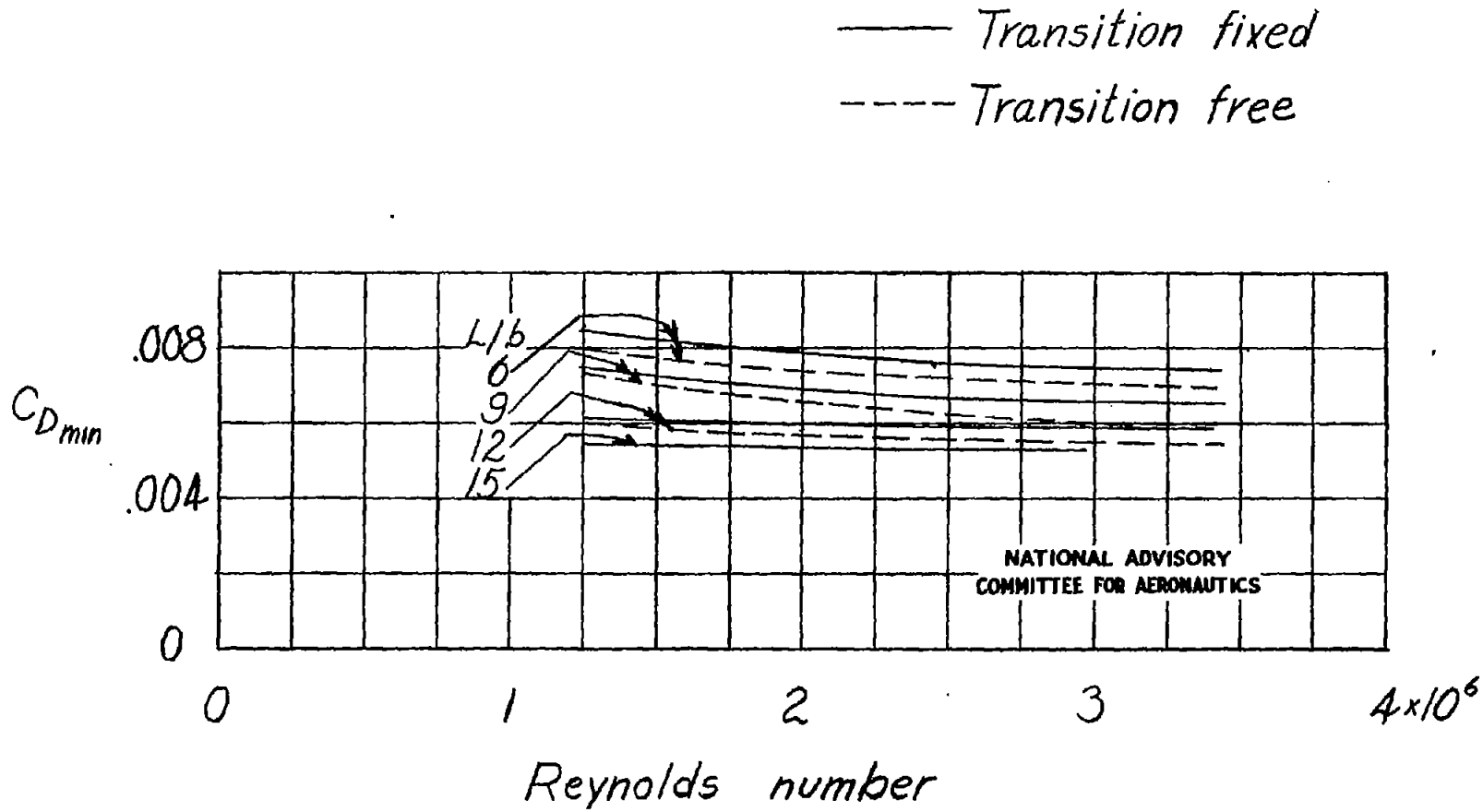

Figure 13.- Effect of Reynolds number on $C_{D_{min}}$ for the $\frac{1}{10}$-scale hulls of a hypothetical flying boat.

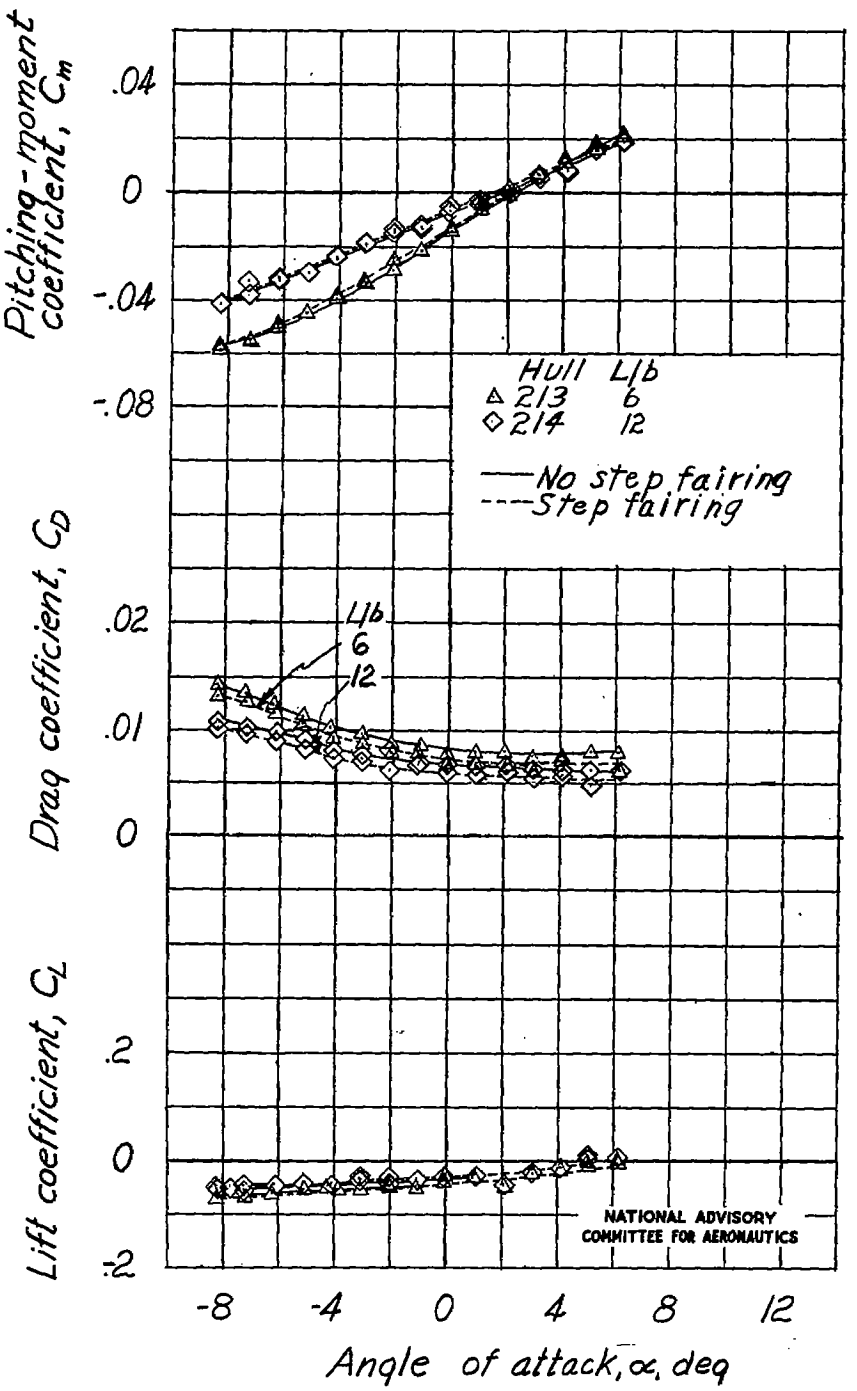

Figure 14.- Effect of step fairing on the aerodynamic characteristics in pitch of the $\frac{1}{10}$-scale hulls of a hypothetical flying boat. R = 2,450,000; transition fixed; three-dimensional mounting.

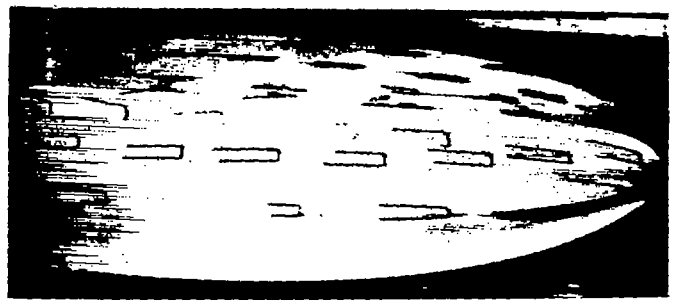

$\alpha = -8^\circ$

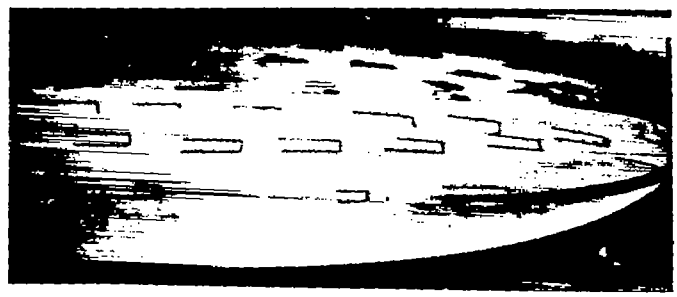

$\alpha = 0^\circ$

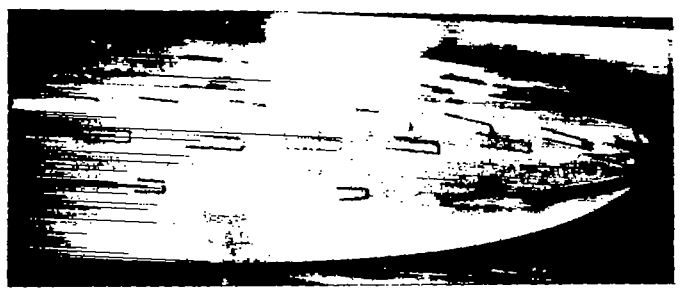

$\alpha = 4^\circ$

$\alpha = 8^\circ$

Figure 15.- Tuft studies of forebody bottom of hull 203 $\left(\frac{L}{b} = 9\right)$.

NATIONAL ADVISORY COMMITTEE FOR AERONAUTICS
LANGLEY MEMORIAL AERONAUTICAL LABORATORY - LANGLEY FIELD, VA

$\alpha = -8^\circ$

$\alpha = 0^\circ$

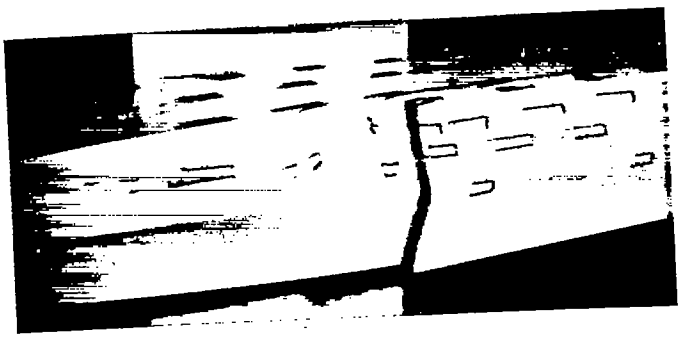

$\alpha = 4^\circ$

$\alpha = 8^\circ$

Figure 16.- Tuft studies of step part of hull 203 $\left(\frac{L}{b} = 9\right)$.

NATIONAL ADVISORY COMMITTEE FOR AERONAUTICS
LANGLEY MEMORIAL AERONAUTICAL LABORATORY - LANGLEY FIELD, VA.